NAG5-10796

Aeronomy of Ice in the Mesosphere (AIM)

Hampton University
LASP, University of Colorado
Naval Research Laboratory
Space Dynamics Laboratory, Utah State University
Orbital Sciences Corp.
GATS Inc.
Geophysical Institute, University of Alaska Fairbanks

Small Explorer Program
Aeronomy of Ice in the Mesosphere
(AIM)

Science Requirements

Document No. AIM-T-0800 Date: September 27, 2003

Revisions

Rev	Description of Change	By	Approved	Date
A	RELEASED			
B	Post-SRR Baseline			
D	Post CCSRR Baseline	SB		09/27/03

Table of Contents

Scope of the Document

This document defines the science requirements for the *AIM* mission. These science requirements provide the basis from which engineering requirements are derived for the mission, spacecraft and instruments. The science requirements are also referenced in the Mission Requirements and Definition, which serves as the basis for mission assessments conducted by NASA during the development period and provides the baseline for the determination of the science mission success during the operational phase.

The baseline *AIM* mission will launch in 2006 and shall determine why polar mesospheric clouds form and why they vary. In the context of this document, statements using the word "**shall**" are mandatory requirements for the mission to be verified. Statements using the words "**is**" or "**will**" are descriptive and provide information relevant to understanding the requirements, but are not themselves requirements subject to verification. Statements using the word "**should**" indicate goals for which a best effort shall be made. Goals are stated for the purpose of clarifying desired performance and are not to influence the allocation of mission resources.

1 Baseline and Minimum Science Requirements

The overall goal of the Aeronomy of Ice in the Mesosphere (AIM) experiment is to resolve why Polar Mesospheric Clouds form and why they vary. By measuring PMCs and the thermal, chemical and dynamical environment in which they form, we will quantify the connection between these clouds and the meteorology of the polar mesosphere. In the end, this will provide the basis for study of long-term variability in the mesospheric climate and its relationship to global change. The results of AIM will be a rigorous validation of predictive models that can reliably use past PMC changes and present trends as indicators of global change. The AIM goal will be achieved by measuring PMC extinction, brightness, spatial distribution, particle size distributions, gravity wave activity, dust influx to the atmosphere and precise, vertical profile measurements of temperature, H_2O, CH_4, O_3, CO_2, NO, and aerosols. These data can only be obtained by a complement of instruments on an orbiting spacecraft (S/C).

The baseline AIM mission will obtain the following measurements:

1) For a sample of high latitude locations distributed in time throughout two northern and two southern PMC seasons, AIM shall obtain altitude profiles of H_2O, Temperature, O_3, CH_4, CO_2, NO, and aerosols in the altitude range 75 to 85 km with an altitude resolution of at least 2 km.

2) For the PMCs located in the above profiles, AIM shall determine the brightness, extinction coefficient, and mean particle size.

3) AIM shall obtain nadir UV images for latitudes greater than 30 degrees with a spatial resolution of at least 2 km to determine the distribution and structure of PMCs.

4) AIM shall determine the daily influx of cosmic dust particles.

As a minimum the AIM mission shall accomplish the following:

1) For a sample of high latitude locations distributed in time throughout one PMC season (North or South), AIM shall obtain altitude profiles of PMCs, H_2O, Temperature, O_3, CO_2 ,and NO in the altitude range 78 to 85 km with an altitude resolution of at least 3 km.
2) For the PMCs located in the above profiles, AIM shall determine the brightness, extinction coefficient, and mean particle size.

3) AIM shall obtain nadir UV images for latitudes greater than 50 degrees with a spatial resolution of at least 3 km to determine the distribution and structure of PMCs.

2 AIM Science Requirements

In order to achieve the science objectives, the mission requires a complement of science instruments to measure the occurrence rates and geographical distribution of PMCs, the size distribution of PMC particles, cosmic dust influx to the atmosphere and precise, vertical profile measurements of temperature, H_2O, CH_4, O_3, CO_2, NO, and aerosols. These geophysical parameters are measured on AIM by three instruments. These are the Solar Occultation for Ice Experiment (SOFIE), the Cloud Image and Particle Size (CIPS) instrument, and the Cosmic Dust Experiment (CDE). SOFIE observes the atmosphere using the solar occultation technique while CIPS is a nadir viewing atmospheric imager. CDE is a zenith viewing dust collector.

Tables 1 and 2 trace the science objectives through to instrument requirements, spacecraft requirements, and mission design. Table 1 lists the six questions and the geophysical parameters that are required to address them. The geophysical parameters include properties of the clouds, their morphology, the cosmic dust input, and the chemical and dynamical environment in which the clouds form. Required geophysical parameters are identified for each objective. A given geophysical parameter such as temperature may be required to address several of the questions. Some of these geophysical parameters are directly observed while other parameters are determined from an observable with a quantifiable relationship to that parameter. For example water abundance can be directly observed through observation of the altitude profile of H_2O attenuation of sunlight while temperature is determined from the altitude profile of CO_2-attenuation of sunlight. Table 2 connects each required geophysical parameter to the observable that will be used. Each observable is then connected to the instrument that will make that particular observation. This table summarizes the work of the AIM science team in determining what observations are required and which techniques are most appropriate (cost, schedule, risk) for providing the required information. A complete description of the rational for these requirements can be found in Appendix A.

Given the global nature of the observations it is required that AIM fly in a polar sun-synchronous orbit with a noon local time of the ascending node. This orbit maximizes the number of PMC observations by SOFIE. In order to discern differences between PMCs in the northern and southern hemispheres and to minimize the effects of inter-annual variability, the AIM baseline mission is to observe two PMC seasons in each hemisphere.

The requirements on observations and the selection of observation techniques (instruments) lead to several mission level requirements. A critical requirement is that observations by the two atmospheric observing instruments (SOFIE and CIPS) must be made in one common volume of air at least once each orbit. This requirement is crucial since only the two instruments together can provide both the properties of an individual cloud as well as the environment in which the cloud formed. While one common volume of air must be observed by both instruments each orbit, it is not required that both observations be made at the same time. The observations may be made as much as 12 minutes apart. Because SOFIE observations are only made once per orbit in each hemisphere, the common volume is defined by the location of the SOFIE occultation measurement. Thus the requirement for common volume measurements effectively means that the SOFIE occultation location must be contained within CIPS images each orbit. CIPS must be able to resolve the SOFIE slit-image with at least two resolution elements within its images.

For an ideal noon-midnight orbit, SOFIE observations are always in the orbit plane and nadir viewing CIPS images will always contain the location of those observations. In practice, SOFIE observations will not be in the orbit plane due to variations in the orbit β-angle that are caused both naturally and due

to orbit insertion errors. Natural variations of the β-angle are on the order of +/- 5 degrees in accordance with the equation of time. The β-angle may be increased if the orbit inclination is not nominal. This would result in a precession rate different from 360 degrees per 365 days. The maximum that the orbit may be allowed to deviate over the mission from noon / midnight is +/- 9 degrees in β-angle. The requirement for common volume observations affects requirements on the CIPS field-of-regard, the maximum errors in orbit inclination, and the pointing capability and knowledge of the spacecraft.

The requirement for data availability is derived from the need to observe PMC behavior at the beginning and ends of the PMC seasons. At these times, there is typically a sharp rise (or fall) in PMC formation over a period of about 5 days. To ensure that AIM observes a minimum number of common volume measurements needed to understand the rapid changes during these periods, it has been determined that 60% of the possible observations in any 5 day period must be obtained and successfully transmitted.

At any time during the PMC seasons, the observations of the common volume are the highest priority. These data include both the SOFIE and CIPS observations of the common volume and all CIPS data taken between the two observations. CIPS data taken outside of the common volume observations are important but of a secondary importance to the common volume observations. Outside the PMC seasons, no observations are required in order to address AIM objectives.

The full list of requirements is tabulated in Table 3. This table connects each requirement to the science questions from which they are derived. Included in this table are goals where applicable. As stated earlier goals are listed for information purposes and are not meant to be drivers for resource allocations or design effort. Table 3 also includes identification numbers for each requirement to be used in requirements tracking and verification.

Table 1. Science Objectives Traceability to Instruments

Science Objectives Determine the Required Geophysical Parameters to be Measured
Required Geophysical Parameters Dictate the Necessary Observations which then Define the Required Instruments

1. What is the global morphology of PMC particle size, occurrence frequency and dependence upon H_2O and Temperature?	2. Do GW enhance PMC formation by perturbing the required temperature for condensation and nucleation?	3. How does dynamical variability control the length of the cold summer mesopause season, its latitudinal extent and possible interhemispheric asymmetry?	4. What are the relative roles of gas phase chemistry, surface chemistry, condensation, sublimation and dynamics in determining the variability of H_2O in the polar mesosphere?	5. Is PMC formation controlled solely by changes in the frost point or do extra-terrestrial forcings such as cosmic dust influx or ionization sources play a role?	6. What is needed to establish a physical basis for the study of mesospheric climate change and its relationship to global change?		Instruments
Geophysical Parameters Needed to Address the AIM Science Objectives						Observables	
PMC Morphology Particle Sizes	PMC Morphology	PMC Morphology	PMC Morphology	PMC Morphology	Objective 6 is addressed through the results of the previous objectives.	Cloud Extinction	SOFIE
Temperature Profile		T, CO_2 Profiles Circulation	Temperature Profile	Temperature Profile		CO_2 Absorption	
H_2O Profile		H_2O Profile Circulation	H_2O Profile	H_2O Profile		H_2O Absorption	
			O_3 Profile			O_3 Absorption	
		CH_4 Profile Circulation	CH_4 Profile Circulation			CH_4 Absorption	
		PMC Morphology, Global Images GW Activity		Ionization NO Profile		NO Absorption	
PMC Morphology, Global Images PMC Particle Sizes	PMC Morphology, Global Images GW Activity		PMC Morphology, Global Images	PMC Morphology, Global Images		Scattered Sunlight	CIPS
				Cosmic Dust Influx		Cosmic Dust Influx	CDE

Table 2. Observables Traceability to Instruments

Technique	Observables	Geophysical Parameters	SRD Instrument (Observation) Requirements[1]	
SOFIE	Cloud Extinction	PMC Morphology Part Sizes	Alt. Range (km)	78 - 85
			Vert. Resolution	3 km
			Horiz. Resolution	At common vol.
			Temp. Resolution	1 min.@ com. vol.
			Precision	$5x10^{-6}$ km^{-1}
	CO_2 Absorption	Temperature	Alt. Range	70 - 90
			Vert. Resolution	3 km
			Horiz. Resolution	5 deg x 24 deg lat x lon
			Temp. Resolution	1 min.@ com. vol.
			Precision	5 K
	H_2O,O_3,CH_4, CO_2, NO Abs.	Mixing Ratio Profiles, Circulation	Alt. Range (km)	78-90, 78-90, 30-90, 80-100,80-95
			Vert. Resolution	3, 3, 3, 3, 5 km
			Horiz. Resolution	5 deg x 24 deg lat x lon
			Temp. Resolution	1 day (1 min O_3)
			Precision (ppmv)	0.6, 0 .1, 0.05, 10.0, 1 x 10^7 cm^{-3}
CIPS	Scattered Sunlight	PMC Morph. Particle Sizes	Alt. Range (km)	Cloud heights
			Vert. Resolution	N/A
			Horiz. Resolution	0.5 deg x 1 deg lat x lon
			Temp. Resolution	1 min
			Precision	16%, 50%
CDE	Cosmic Dust Influx	Cosmic Dust Influx	Alt. Range (km)	Cloud alt
			Vert. Resolution	N/A
			Size range	$r < 0.7$ μm
			Temp. Resolution	1 week
			Precision	10%

[1]Precisions are quoted at cloud height.

Table 3: AIM Science Requirements

Science Question	Geophysical Parameter / Observable	ID	Observation Property	Requirement	Goal
All (Mission Level Requirements)	Orbit	SCI139	Orbit Type	Polar, sun-synchronous	n/a
	Orbit	SCI140	Local time of ascending node	Noon +/- 36 arcmin (9 degrees)	Noon +/- 20 arcmin (5 degrees)
	Observations	SCI141	Common Volume	CIPS and SOFIE shall observe at least one common volume of air each orbit	n/a
	Observations	SCI246	Common Volume	CIPS must resolve the SOFIE slit image each orbit with at least 2 resolution elements	CIPS must resolve the SOFIE slit image each orbit with at least 4 resolution elements
	Observations	SCI142	Temporal Separation	Common volume observations shall be separated in time by no more than 12 minutes	Common volume observations shall be separated in time by no more than 6 minutes
	Observations	SCI143	Temporal Extent	Observe two PMC seasons in each hemisphere	n/a
PMC Microphysics	PMC Presence Scattered Sunlight	SCI45	Horizontal extent (latitude range within measurements are required)	55-80 degrees	30-80 degrees
	PMC Presence Scattered Sunlight	SCI46	Temporal Resolution (maximum integration period	10 seconds	5 seconds
	PMC Presence Scattered Sunlight	SCI47	Temporal extent (period over which measurements are taken):	solstice+2 weeks, +/- 7 weeks.	solstice+2 weeks, +/- 10 weeks.
	PMC Presence Scattered Sunlight	SCI48	Accuracy for nadir Albedo Ratio (AR):	10	2
	PMC Presence Scattered Sunlight	SCI49	Precision for nadir Albedo Ratio (AR):	100%.	33%
	PMC Presence / Extinction Coefficient at 3 mm	SCI50	Minimum detection threshold:	5x10-5 km-1	5x10-7 km-1 at 3 micrometers
	PMC Presence / Extinction Coefficient at 3 mm	SCI51	Vertical resolution:	3 km	1 km
	PMC Brightness / Scattered Sunlight	SCI52	Accuracy	15% for clouds with AR > 5	15% for clouds with 2 < AR < 5
	PMC Brightness / Scattered Sunlight	SCI53	Precision:	5% for clouds with 5 < AR < 50	5% for clouds with 2 < AR < 50

Science Question	Geophysical Parameter / Observable	ID	Observation Property	Requirement	Goal
	PMC Brightness / Extinction Coefficient at 3 mm	SCI54	Accuracy	15% for clouds with extinction, k > 2x10-4 km-1	15% for clouds with extinction 5x10-5 < km-1 < 2x10-4 km-1
	PMC Brightness / Extinction Coefficient at 3 mm	SCI55	Precision	5% for clouds with extinction, k > 2x10-4 km-1	5% for clouds with extinction 5x10-5 < km-1 < 2x10-4 km-1
	PMC Particle Sizes / Scattered Sunlight	SCI56	Specific spatial	< 10 deg	< 3 deg
	PMC Particle Sizes / Scattered Sunlight	SCI57	Accuracy	50%	
	PMC Particle Sizes / Scattered Sunlight	SCI58	Precision	10%	
	Water Vapor	SCI59	Accuracy	1.5 ppmv	0.5ppmv
	Water Vapor	SCI60	precision	0.75 ppmv	0.3 ppmv
	Temperature	SCI61	accuracy	5 K	2K
	Temperature	SCI62	precision	1K	0.5K
Gravity Wave Effects	PMC Morphology / Gravity Wave Occurrences	SCI63	Altitude	PMC Altitudes	
	PMC Morphology / Gravity Wave Occurrences	SCI64	Horizontal wavelengths	> 20 km.	
	PMC Morphology / Gravity Wave Occurrences	SCI65	Horizontal resolution	3 km.	2 km
	Nadir UV Images	SCI66	Time spacing	1 image set per 60 seconds	1 image per 10 seconds
	Nadir UV Images	SCI67	Precision for geographic location of nadir images	+/- 5 km.	+/- 2 km
	Nadir UV Images	SCI68	Measurement temporal resolution (maximum integration time)	0.4 sec.	0.2 sec
	Temperature	SCI69	Altitude range	81-85 km.	75 – 95 km
	Temperature	SCI70	Vertical resolution	3 km.	1 km
	Temperature	SCI71	Horizontal resolution	500 km.	150 km
	Temperature	SCI72	Temporal resolution	1 day.	1 min.
	Temperature	SCI73	Accuracy	+/- 5 K.	+/- 1 K
	H2O mixing ratio	SCI74	Altitude range	81-85 km.	75 – 95 km
	H2O mixing ratio	SCI75	Vertical Resolution	3 km.	1 km
	H2O mixing ratio	SCI76	Horizontal resolution	500 km.	150 km
	H2O mixing ratio	SCI77	Temporal resolution	1 day	1 min.

Science Question	Geophysical Parameter / Observable	ID	Observation Property	Requirement	Goal
Temperature Variability	Temperature	SCI78	Accuracy	5 K	2K
	Temperature	SCI79	Precision	< 5 K	<2K
	Temperature	SCI80	Vertical resolution	4 km.	2 km
	Temperature	SCI81	Temporal resolution	4 days	1 day
	Temperature	SCI82	Longitudinal resolution	45 deg	Long-Lat resolution of 5 deg x 2 deg.
	CH4 & H2O Mixing Ratio	SCI83	Accuracy	1 ppmv	<0.5
	CH4 & H2O Mixing Ratio	SCI84	Precision	1 ppmv	<0.5
	CH4 & H2O Mixing Ratio	SCI85	Vertical resolution	4 km.	2 km
	CH4 & H2O Mixing Ratio	SCI86	Temporal resolution	1 week	1 day
	CH4 & H2O Mixing Ratio	SCI87	Longitudinal resolution	45 deg	Long-Lat resolution of 10 deg x 2 deg.
Hydrogen Chemistry	CH4, H2O & Temperature	SCI88	Altitude range	50-85 km.	
	CH4, H2O & Temperature	SCI89	Vertical resolution	3 km	2 km
	CH4, H2O & Temperature	SCI90	Longitudinal resolution	20 degrees	15 deg
	CH4, H2O & Temperature	SCI91	Temporal resolution	2 hours.	1.5 hours
	CH4, H2O & Temperature	SCI92	Accuracy	20%.	10%
	CH4, H2O & Temperature	SCI93	Precision	10%.	5%
	Heterogeneous Chemistry / O3, H2O & Temperature	SCI94	Altitude range	50-85 km.	
	Heterogeneous Chemistry / O3, H2O & Temperature	SCI95	Vertical resolution	3 km vertical resolution.	2 km
	Heterogeneous Chemistry / O3, H2O & Temperature	SCI96	Longitudinal resolution	20 degrees	15 deg

Science Question	Geophysical Parameter / Observable	ID	Observation Property	Requirement	Goal
	Heterogeneous Chemistry / O3, H2O & Temperature	SCI97	Temporal resolution	2 hours	1.5 hours
	Heterogeneous Chemistry / O3, H2O & Temperature	SCI98	Accuracy	20%	10%
	Heterogeneous Chemistry / O3, H2O & Temperature	SCI99	Precision	10%	5%
PMC Nucleation Environment	PMC Morphology / Scattered Sunlight	SCI100	Altitude range	81-85 km	75 – 95 km
	PMC Morphology / Scattered Sunlight	SCI101	Vertical resolution	3 km	1 km
	PMC Morphology / Scattered Sunlight	SCI102	Horizontal resolution	500 km	150 km
	PMC Morphology / Scattered Sunlight	SCI103	Temporal resolution	1 min.	12 sec
	PMC Morphology / Scattered Sunlight	SCI104	Precision	56%.	2%
	Temperature	SCI105	Altitude range	81-85 km	75 – 95 km
	Temperature	SCI106	Vertical resolution	3 km	1 km
	Temperature	SCI107	Horizontal resolution	500 km	150 km
	Temperature	SCI108	Temporal resolution	1 day	1 min
	Temperature	SCI109	Precision	+/-5 K	+/- 1 K
	Water Vapor	SCI110	Altitude range	81-85 km	75-95 km
	Water Vapor	SCI111	Vertical resolution	3 km	1 km
	Water Vapor	SCI112	Horizontal resolution	500 km	150 km
	Water Vapor	SCI113	Temporal resolution	1 day	1 min.
	Water Vapor	SCI114	Precision	50%	10%
	Water Vapor	SCI115	Altitude range	80-95 km	80 – 130 km
	Nitric Oxide	SCI116	Altitude range	80-95 km	80 – 130 km
	Nitric Oxide	SCI117	Vertical resolution	5 km	1 km
	Nitric Oxide	SCI118	Horizontal resolution	500 km	100 km
	Nitric Oxide	SCI119	Temporal resolution	1 day	1 hour
	Nitric Oxide	SCI120	Precision	1x105 cm-3	1x107 cm-3
	Cosmic Dust	SCI121	Altitude	Spacecraft altitude	
	Cosmic Dust	SCI122	Precision	10% for dust sizes < 0.7 micrometers	10% for < 0.2 micrometers
	Cosmic Dust	SCI123	Temporal resolution	1 week	1 day

Science Question	Geophysical Parameter / Observable	ID	Observation Property	Requirement	Goal
Long-Term Mesospheric	PMC Limb Brightness / Extinction	SCI124	Altitude range	81-85 km	75-95 km
	PMC Limb Brightness / Extinction	SCI125	Vertical resolution	3 km	1 km
	PMC Limb Brightness / Extinction	SCI126	Horizontal resolution	500 km	
	PMC Limb Brightness / Extinction	SCI127	Precision	15%	10%
	PMC Limb Brightness / Extinction	SCI128	Temporal resolution	1 min	12 sec
	Water Vapor	SCI129	Altitude range	81-85 km	75-95 km
	Water Vapor	SCI130	Vertical resolution	3 km	1 km
	Water Vapor	SCI131	Horizontal resolution	500 km	150 km
	Water Vapor	SCI132	Temporal resolution	1 day	1 min
	Water Vapor	SCI133	Precision	50%	10%
	Temperature	SCI134	Altitude range	81-85 km	75-95 km
	Temperature	SCI135	Vertical resolution	3 km	1 km
	Temperature	SCI136	Horizontal resolution	500 km	150 km
	Temperature	SCI137	Temporal resolution	1 day.	1 min.
	Temperature	SCI138	Precision	+/- 5 K	+/- 1 K

3 Appendix A. Rational for Science Requirements

The overall goal of the Aeronomy of Ice in the Mesosphere (AIM) experiment is to resolve why PMCs form and why they vary. By measuring PMCs and the thermal, chemical and dynamical environment in which they form, we will quantify the connection between these clouds and the meteorology of the polar mesosphere. In the end, this will provide the basis for study of long-term variability in the mesospheric climate and its relationship to global change. The results of AIM will be a rigorous validation of predictive models that can reliably use past PMC changes and present trends as indicators of global change. This goal will be achieved by measuring PMC abundances, spatial distribution, particle size distributions, gravity wave activity, dust influx to the atmosphere and precise, vertical profile measurements of temperature, H_2O, OH, CH_4, O_3, CO_2, NO, and aerosols. These data can only be obtained by a complement of instruments on an orbiting spacecraft (S/C).

The purpose of this appendix is to specify the individual objectives of the AIM mission and to list the measurements required for answering those objectives. The analysis that will occur for each measurement is discussed so that for each measurement, the spatial resolution, accuracy, and precision requirements are specified. For each requirement, a goal is listed as well as a minimum. The purpose of including minimum requirements and goals is to specify both those measurements that will ensure an answering of the science objectives as well as those that add even more to the science return. For each objective, a tabulated list of required geophysical parameters is presented along with the requirements on the measurements of those geophysical parameters.

For the purposes of this appendix, we will define the precision of any measurement as root sum square of all of the known random components to the uncertainty in that measurement. The accuracy of any measurement is the root sum square of all of the known random and known systematic components to the uncertainty of that measurement.

4 Objective 1. PMC Microphysics

4.1 Science Question:

What is the global morphology of PMC particle size, occurrence frequency and dependence upon H_2O and temperature?

The simplest model of PMC formation presumes the existence of supersaturated conditions; however, even this most basic assumption has not been validated because we lack comprehensive data on the relative humidity of the polar mesopause region and its association with PMC occurrence. More detailed microphysical modeling suggests that after nucleation, the cloud particle eventually grows large enough that it falls into a region of warmer temperatures where it sublimates. It has been suggested that the resultant evaporated H_2O can be then relofted into the region of cold temperatures where the condensation / growth / decay process cyclically repeats. Sugiyama [1996] has postulated that an apparent periodicity in the strength of PMSE is consistent with this view. One signature of this process would be a layer of enhanced H_2O lying just below the cloud layer; indeed we may have already detected such a layer. The cycling time is also sensitive to the particle size; large particles would fall more quickly and would require higher H_2O abundances to form. They would also need stronger upwelling rates to remain buoyant long enough to grow.

Statistical studies of H_2O/T/PMC correlations will be invaluable in validating various microphysical scenarios. The possible correlation of PMCs with either H_2O or temperature will allow us to isolate which of the two is the key driver for cloud formation. We will also be able to estimate the amount of water taken up in clouds and compare this with the measured cloud densities and particle sizes.

4.2 Required Geophysical Parameters

An operational definition of "microphysics" is the relationship of PMC properties to the forcing variables of water vapor, temperature, nucleating dust particles, vertical wind, etc. AIM, in principle, will be able to provide this relationship over certain scale sizes and at certain instants of time. The ultimate goal is to be able to extend this relationship to situations where the forcing variables are known, or in other words, to use it in a predictive way. For example, it could be used in models of global atmospheric change to predict how global-scale PMC coverage would change as a function of the forcing variables. Perhaps a more immediate goal is the reverse – to be able to make a statement about the changed environment, if the PMCs are found to change over time (e.g., in their seasonal or spatial characteristics). This will be most helpful in trying to understand what happened over the past 116 years of PMC history. To determine the appropriate spatial and temporal resolution required by the AIM measurements for this objective, we must thus consider the spatial and temporal scales on which we expect variations in PMCs, and on which we need to correlate PMCs with forcing variables such as H_2O or temperature in order to understand PMC microphysical processes. The goal here is to obtain observations which are appropriate for testing the microphysical models, such as CARMA. Although gravity waves perturb PMC distributions and morphology, we believe that the larger-scale planetary waves, and the slow variations of the background fields with latitudes and season, are the appropriate scales on which to base our investigations of microphysics.

4.2.1 PMC Presence

Evaluating the presence and occurrence frequency of PMC concerns only individual measurements of clouds, and is not complicated by requirements of correlated measurements (e.g., either between different instruments, or between different measurements by the same instrument). Nor does it benefit from the possibility of averaging observations over large spatial or temporal scales. To achieve this objective, at a minimum, we require clear separation of cloudy and cloud-free regions. Thus, our minimum resolution element must be the size of the overall clouds themselves, which typically have lateral extents of several hundred km. The minimum horizontal resolution is **400 km**, with a goal of **50 km**, so that the edge regions are fairly well defined. Note that these requirements refer to single measurements (e.g., one pixel or group of pixels for a nadir view, the line-of-sight or horizontal fov for a limb view) and the specified resolution indicates the amount of area over which a measurement can be smeared. At a minimum, clouds must be observed in at least two different hemispheres (E and W), each day. The goal is to obtain measurements with continuous longitudinal coverage (this could be achieved by the nadir view) over the course of a day. Further, since the PMC region is known to extend to at least 55° in latitude, measurements must be acquired from 55° to 80° in the summer hemisphere – there is no requirement for continuous coverage over this region; this simply specifies the range of latitudes within which measurements are required. Our goal is to obtain measurements from 30° to 80° in the summer hemisphere, to ensure that the PMC edge region is detected. There is another requirement levied on the nadir viewing instrument. The nadir images will be used to supply information to the limb viewers about the presence of clouds along their lines of sight. For this purpose, we require a minimum horizontal resolution of **50 km**, with a goal of **10 km** (see Figure 1.1).

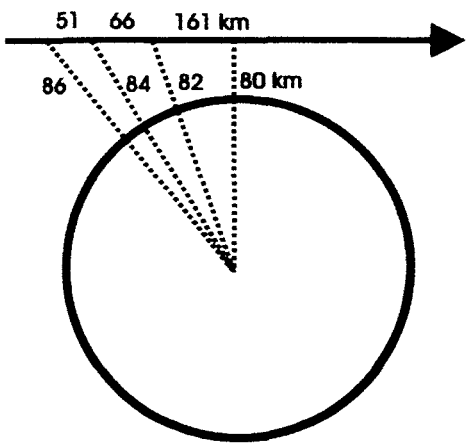

Figure 1.1 Limb viewing path lengths through PMCs.

We require that we "freeze" the clouds in space, so their existence and position is not perturbed significantly on the 50-400 km scale defined above. Thus, our definition of the required temporal resolution must satisfy the concept of a "frozen" cloud. There are several different time scales to consider here, e.g., evaporation of the PMC particles, translation by the mean wind, and satellite motion. Clouds typically persist for hours to several days [Thomas, 1991], but will be translated by the mean wind at speeds of 10-100 m/s [Haurwitz and Fogle, 1969]. The satellite, however, is moving at a rate of 8 km/s at ~500 km altitude. Thus, the satellite motion is the limiting factor in determining the required temporal resolution for individual observations. Our minimum temporal resolution for a single "snapshot" of a cloud is thus **10 seconds** (FOV moves ~30% of a typical cloud extent along the satellite track), with a goal of **2 seconds** (FOV moves about 30% of 50 km). As for horizontal resolution, these requirements refer to individual measurements.

The vertical resolution requirement pertains only to limb viewing measurements, since nadir images of PMCs are vertically unresolved. From past limb observations (e.g., POAM, SME, WINDII) we know that PMCs have vertical widths of about 1-2 km, so the goal and minimum here are about **1 km** and **3 km**, respectively.

The required accuracy and precision of a PMC detection is determined by the threshold brightness, below which a cloud cannot be reliably distinguished from the background Rayleigh scattering signal. This threshold is defined differently for nadir-viewing and limb-viewing instruments, so we discuss these cases separately.

Limb view: Occultation.

We examine the accuracy of the limb occultation measurements in terms of the extinction. Our requirements are based on the measurements made by HALOE, which is itself a solar occultation instrument. Typical PMC extinctions measured by HALOE were around 10^{-4} km^{-1} at 3 μm, which is near the peak PMC absorption wavelength. HALOE detected sufficient clouds to constitute a statistical data base for microphysical studies, so we place our minimum threshold at slightly lower than the typical cloud extinction, or **$5x10^{-5}$ km^{-1} at 3 μm**. This corresponds to a significantly smaller threshold for other channels (e.g., $1.5x10^{-7}$ km^{-1} at 2.4 μm). For obtaining the most complete morphology of PMCs, we will view PMCs that are much dimmer than the "typical" clouds detected by HALOE. Thus, we set our goal at **$5x10^{-7}$ km^{-1} at 3 μm**.

Nadir view.

For the nadir view, we base our estimates on the simulation of UV albedos as a function of solar zenith angle (Figure 1.2). Our minimum requirement is to detect clouds that correspond to model C (intermediate to high brightness class from SME), with a goal of detecting clouds that fall on the model B curve (relatively low PMC brightness). We further assume that the necessary measurements for testing the microphysical model will be obtained only in the common volume regions of the limb and nadir instruments, which limits the observations to the region near SZA=90. We examine the cloud+background albedo divided by background albedo, which we call "AR" for Albedo Ratio. For Model C at 90° SZA, this is $\sim 10^{-4}/10^{-5} = \mathbf{10}$. For Model B at 90°, this is $\sim 2x10^{-5}/1x10^{-5} = \mathbf{2}$.

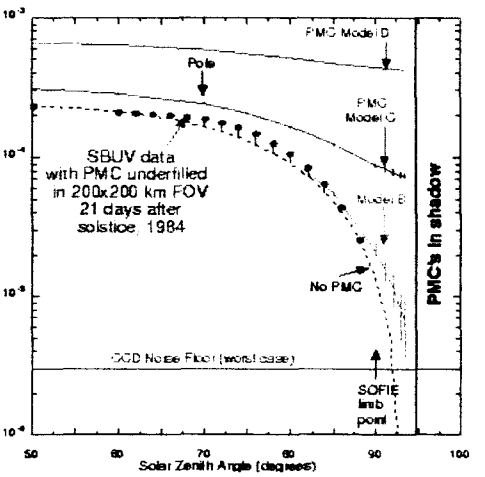

Figure 1.2 AIM proposal figure 2-6: Simulated UV albedos (for 2x2 km pixel) as a function of SZA. The dotted lines represent the UV albedo when no PMCs are present. The dashed lines represent the UV albedo when PMCs are present at optical depths observed by SME. The difference between the solid and the dotted curves are then the difference between CIPS PMC and background signals.

Since the above discussion focuses on the ratio of cloud measurements to measurements of cloud free conditions and we are only checking whether a value exceeds a given threshold, the required precision for each measurement is straightforward to determine. To be able to identify a cloud with AR = 2 as a cloud occurrence (AR>1) within the 2 sigma measurement error requires a precision of ~33% for both albedo values (cloud, clear air).

4.2.2 *PMC Brightness*

We will not only correlate the presence/absence of clouds with PMC forcing variables, but also determine the morphology of the cloud brightness. This parameter is essentially an enhancement to, or an increase in sensitivity over, the presence determination, and will be used to refine the correlations with temperature and water vapor (and will also be used to correlate with GW, although that is not specifically part of this objective). Determining the PMC brightness implies characterizing the intensity of the PMC signal as a function of geographic location and time. The spatial and temporal resolution are the same as the occurrence measurement, for the same reasons.

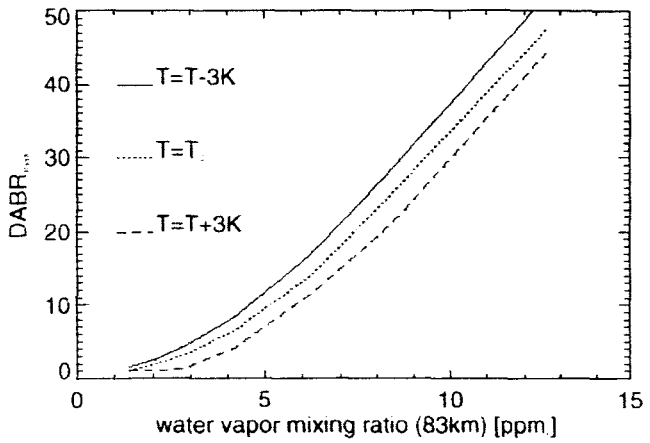

Figure 1.3. The Domain Averaged Backscatter Ratio (DABR) for PMC, as calculated by a 1D model for different values of water vapor mixing ratio and temperature. This plot is used as an example of the correlation between PMC brightness and temperature or water vapor.

Our goal is to statistically correlate the forcing variables (e.g., H_2O, Temperature) with PMC brightness. We define our minimum accuracy and precision by including in our analyses only the brightest clouds. Our goals are then defined to include even the dimmer clouds. To determine the accuracy of the brightness measurements, we base our estimates on microphysical model results correlating H_2O and temperature with brightness (Figure 1.3). These results reveal that over the range of forcing incorporated into the model (2-12 ppmv), the PMC brightness is predicted to vary by a factor of about 20 in a nearly linear fashion. At any given value of H_2O, a variation in the temperature by +(−) 3 K yields a change in brightness of about −(+) 15 to 30%. To reproduce such a correlation curve with our observations, we thus require accuracy in the brightness data of ~15%, and a precision of about 5%. Like we did for PMC presence, we describe the accuracy requirements in terms of both a limb view and a nadir view.

Limb view: Occultation. Based on HALOE observations, typical PMCs have extinctions (k) of about 10^{-4} km^{-1} at 3 μm. Clouds were detected with extinctions that were four to five times larger than this, and the threshold was about a factor of three lower (e.g., detections covered a range of about $3x10^{-5}$ to $5x10^{-4}$ km^{-1}). Thus, for limb occultation measurements, we impose a minimum accuracy (precision) requirement of **15% (5%)** for clouds with $\mathbf{k>2x10^{-4}\ km^{-1}}$, and a goal of **15% (5%)** for clouds with $\mathbf{5x10^{-5}<k<2x10^{-4}\ km^{-1}}$.

Nadir view: As before, we define the accuracy requirements for the nadir view in terms of the albedo ratio, AR. Based on Figure 1.2 above, we define the "bright" cloud threshold to correspond to mid-way between case B and C, or AR at 90° SZA greater than 5. We thus impose a minimum accuracy (precision) requirement of **15% (5%)** for clouds with **AR > 5**, and a goal of **15% (5%)** for clouds with **2 < AR < 5**.

4.2.3 Particle Size

Particle sizes will be inferred from CIPS measurements of PMC brightness vs. scattering angle. They will be determined for the brightest clouds to generate a morphology, and to include along with other measured parameters, such as water vapor and temperature, in microphysical models. Thus, we are interested in particle sizes at locations in the common volumes measured by both the nadir and limb instruments as well as at locations only observed by CIPS. This parameter has many similarities to the brightness requirements pertaining to PMC morphology and H_2O or temperature correlations. There are also other considerations because particle sizes are derived from a series of measurements.

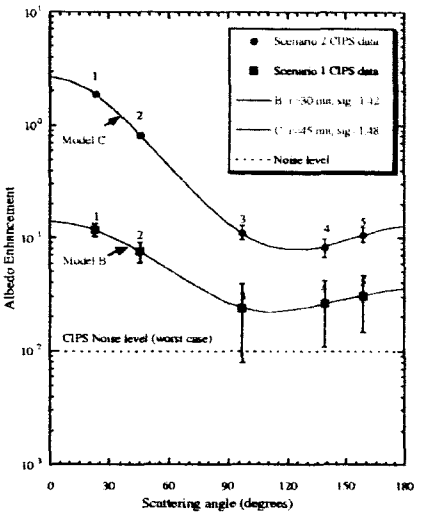

Figure 1.4. AIM proposal figure 2-7: Synthetic CIPS albedo enhancement of a cloud element as seen from 2 SME brightness classes [Thomas, 1995].

The temporal resolution for particle size measurements is the same as for all other measurements above – we require an effectively "frozen" cloud, and are constrained by the S/C motion. The horizontal resolution is also subject to the same considerations as for PMC presence and brightness, but in addition is restricted by other factors. In particular, the scattering angle over which the signals are averaged to attain a specific spatial resolution must be smaller than **10°** as a minimum, and **3°** as a goal. This is necessary since we require a range of scattering angles to calculate the particle size, and particle size information will be lost if the measurements are smeared over too large a range. Another consideration is that we will include in microphysical models the limb instrument measurements of H_2O and temperature as well as the particle size measurements. This assumes that the particle sizes are derived in the same volume of space as observed by the limb instrument. Given in-track (line-of-sight) smearing by the limb instrument, this does not impose requirements any more stringent than the 400km/50km spatial resolutions noted above.

PMC particles are on the order of, to slightly larger than, Rayleigh scattering particles, or about 10-80 nm in diameter assuming spherical shapes. Measuring a distribution of sizes throughout this size range will enable us to quantify particle growth and freeze drying characteristics. For the purposes of enhancing our knowledge of PMC microphysics, we thus require that particles be constrained roughly to 20-nm size bins. That is, we require that our measurements enable us to distinguish between particles that are 10 nm in diameter and 30 nm in diameter, or between 30 and 50 nm, etc. At a minimum, we require that this be accomplished with the brightest clouds; our goal is to determine sizes for the dimmer clouds. Particle sizes will be determined by measuring scattering at a number of different angles by the CIPS instrument. Figure 2-7 from the proposal, included here as Figure 1.4, shows model results for the angular dependence of the particle albedo for two different size distributions with modal radii at 30 nm and 45 nm. To distinguish between these two cases, we require determination of the PMC brightness with an accuracy of **50%** and a precision of **10%**.

4.2.4 Water Vapor

To infer microphysical information from the observations, it will be entirely adequate to correlate H_2O and/or temperature partial column averages over the PMC region. One of the main

considerations is separation of the mesopause (87 km) and PMC altitude regions (82 km). Thus, at a minimum the water vapor measurements need to resolve these two regions, which requires at least **3-km** vertical resolution. Ideally, we would also resolve the PMC, which requires **1-km** vertical resolution. These scales are also consistent with the vertical resolution noted for the PMC observations. Since we wish to correlate H_2O and temperature with the PMC observations, they need to be measured on similar horizontal and temporal scales.

As described above (Figure 1.3), microphysical models predict that the brightness of PMCs will change significantly (by more than a factor of 20) as water vapor mixing ratios at 83 km increase from 2 to 12 ppmv. For the 6 K temperature variation tested by the model, the variation in H_2O at a given PMC brightness is about 1.5 ppmv, and is relatively independent of the water vapor mixing ratio itself. This leads to a suggested accuracy (precision) of at least **1.5 (0.75) ppmv**, with a goal of **0.5 (0.3) ppmv** just to resolve the effect of a 6 K temperature change.

Note that at a minimum, the H_2O correlations with PMCs and/or temperature will include data from an entire season, but may include only a week or even a day when we are investigating the rapid variations at the beginning and ends of the PMC seasons.

4.2.5 Temperature

The same considerations pertain to both the temperature and H_2O measurements, so the required spatial and temporal resolution for the temperature measurements is the same as for the H_2O measurements, as far as microphysics is concerned.

Earlier measurements suggest that temperatures at PMC altitudes are approximately constant at 153±3 K during the primary PMC season, and change by about 5-10 K per week before and after the season. Also, temperatures at PMC altitudes vary by about 2-5 K on diurnal, 2 day, 5 day and 16 day time scales. Thus, to document variations in temperature, and their correlations with PMCs, at a minimum we require **5 K** accuracy (**1 K** precision), with a goal of **2 K** accuracy (**0.5 K** precision).

4.2.6 *Summary of Geophysical Parameters Required for Objective 1*

	PMC Presence		PMC Brightness: Morphology	
	Min	Goal	Min	Goal
Altitude Range (km)	82-83	78-88	82-83	78-88
Vert. Res. (km)	3	1	3	1
Horiz. Res. (km)[1]	*Limb*: 400 *Nadir*: 50	*Limb*: 50 *Nadir*: 10	*Limb*: 400 *Nadir*: 50	*Limb*: 50 *Nadir*: 10
Horiz. Extent[1]	55-80°	30-80°	55-80°	30-80°
Tempo. Res. (sec.)[2]	10	5	10	5
Tempo. Extent[2]	Solstice+2 wks ± 7 wks	Solstice+2 wks ± 10 wks	Solstice+2 wks ± 7 wks	Solstice+2 wks ± 10 wks
Accuracy	*Limb Oc*: $5\times10^{-7}km^{-1}$, 3μm *Nadir*: 10 (AR)	*Limb Oc*: $5\times10^{-5}km^{-1}$, 3μm *Nadir*: 2 (AR)	15% *Limb Oc*: $k>2\times10^{-4}km^{-1}$ *Nadir*: AR>5	15% *Limb Oc*: $5\times10^{-5}<k<2\times10^{-4}km^{-1}$ *Nadir*: 2<AR<5
Precision	*Limb*: 25% *Nadir*: 100%	*Limb*: 5% *Nadir*: 30%	5% *Limb Oc*: $k>2\times10^{-4}km^{-1}$ *Nadir*: AR>5	5% *Limb Oc*: $5\times10^{-5}<k<2\times10^{-4}km^{-1}$ *Nadir*: 2<AR<5

	PMC Brightness: Particle Size		Water Vapor		Temperature	
	Min	Goal	Min	Goal	Min	Goal
Altitude Range (km)	82-83	78-88	82-83	78-92	82-83	78-92
Vert. Res. (km)	N/A	N/A	3	1	3	1
Horiz. Res. (km)[1]	400 (10° sca angle)	50 (3° sca angle)	400	50	400	50
Horiz. Extent[1]	55-80°	30-80°	N/A	N/A	N/A	N/A
Tempo. Res. (sec.)[2]	10	5	10	5	10	5
Tempo. Extent[2]	Solstice+2 wks ± 7 wks	Solstice+2 wks ± 10 wks	Solstice+2 wks ± 7 wks	Solstice+2 wks ± 10 wks	Solstice+2 wks ± 7 wks	Solstice+2 wks ± 10 wks
Accuracy	50% AR>5	50% 2<AR<5	1.5 ppmv	0.5 ppmv	5 K	2 K
Precision	10% AR>5	10% 2<AR<5	0.75 ppmv	0.3 ppmv	1.0 K	0.5 K

[1] The horizontal resolution refers to an individual measurement. The horizontal extent refers to the latitude range within which observations are required. At a minimum, we require measurements at two different longitudes separated by 180°; our goal is to obtain continuous longitudinal coverage. At a minimum we require measurements anywhere within the 55°-80° summer polar region. Our goal is to obtain continuous latitudinal coverage in the nadir from 30° to the 80°in the summer hemisphere.

[2] The temporal resolution refers to an individual measurement. The temporal extent refers to the time frame within which observations are required. At a minimum, we require measurements every two to three days during the time periods specified. Our goal is to obtain measurements every day during the time periods specified

5 Objective 2. Gravity Wave Effects

5.1 Science Question

Do GW enhance PMC formation by perturbing the required temperature for condensation and nucleation?

Internal atmospheric gravity waves (GW) have long been believed to be highly relevant to PMC microphysics. The seasonal change of wave flux at mesopause heights is considered to be the single most important factor in driving the vigorous upwelling and consequent extremely low mesopause temperature environment during the high-latitude summer [Luo et al., 1995; Kirkwood et al., 1998]. Quantitatively, Jensen and Thomas [1994] have suggested that the sublimation of cloud particles in the warm phase of a GW occurred more rapidly than condensation in the cold phase. Thus the presence of GW could lower the temperature required for cloud formation to below the nominal saturation temperature. In contrast, Klostermeyer [1998] concluded that mesospheric cloud condensation could be enhanced by GW. His simulations resemble lidar soundings of NLC, which indicate an important role for GW in shaping NLC formation. Klostermeyer's hypothesis depends upon more H_2O (>6 ppmv) than generally accepted for the mesopause region, as suggested by HALOE data [Siskind, 1998]. This would accelerate the nucleation process to the point where it is comparable to typical GW periods. This could explain the observation of mesospheric clouds in regions where supersaturation is not thought to exist (e.g. recent observations at mid-latitudes over the continental United States; Taylor et al., 2002; Wickwar et al., 2002) and is analogous to processes known to occur with stratospheric mountain waves and Polar Stratospheric Clouds (PSC) [Bacmeister et al., 1999].

AIM will measure gravity wave occurrence and spatial characteristics (geographic location, horizontal wavelength and direction of orientation) at the 80-85 km level by imaging wave patterns in the PMC directly. Simultaneous measurements of mesospheric temperature profile and H_2O content over the same latitude range will be used together with state-of-the art modeling to quantitatively test these hypotheses.

5.2 Required Geophysical Parameters

5.2.1 PMC Morphology

The spectrum of internal gravity waves is very broad and encompasses perturbations with periods ranging from a few minutes to several hours and horizontal wavelengths of a few 10's km to several thousand km. In addition, tides and planetary waves are known to play a major role in defining the instantaneous background atmosphere. The waves that are predominantly seen in ground-based NLC imagery, termed "bands" exhibit periods of typically <1hour and horizontal scales of up to a few hundred km. These relatively short-period waves are now known to be important drivers of the mean flow as they can transport copious amounts of horizontal momentum from the troposphere into the upper atmosphere. However, their influence on PMC formation has yet to be quantified. Much smaller scale, spatially localized, wave patterns termed "billows" are also common in NLC displays. These waves are thought to be generated in situ by a Kelvin-Helmholtz shear, or a convective-type instability but due to their transient nature (lifetimes several min.) they are not considered to play any significant role in the large-scale PMC formation process. In contrast, the longer period gravity waves, tides, planetary waves are expected to play an extremely important role in PMC formation, as their periodicities/lifetimes are more akin to the expected PMC growth time (according to current theories). The CIPS instrument will measure the GW bands and the longer period wave content at the 80-85 km level by imaging them directly in the PMC field and by long base-line photometry as utilized by Carbary et al., [2000].

Our goal is to measure GW of horizontal wavelengths >20 km and lifetimes of a few hours. To clearly resolve these waves in the nadir would require a minimum spatial resolution of ~ 4-5 km. However, this would result in unacceptably large pixel footprints (similar to the horizontal scale sizes of shorter period GW) near the edge of the CIPS field of view. A minimum requirement of 3-km pixel resolution in the nadir is therefore advocated (with a goal of 2 km to improve off nadir image definition).

Due to the rapid motion of the spacecraft we will not be able to measure the speed of the GW. However, measurements of the GW orientation will provide key information on their propagation direction (with a 180° ambiguity). CIPS will therefore operate in a "snap-shot" mode to obtain large-field overlapping image montages to document accurately the GW morphology and PMC occurrence over the polar region. As gravity waves can exhibit horizontal phase speeds of typically up to 100 m/s a minimum resolution of 1 image set/min would permit accurate mapping of overlapping fields. (A goal of 1 image set/10 sec would facilitate multiple snapshots at different viewing angles for possible tomographic reconstruction of PMC and GW altitudinal profiles.)

A measurement precision of ± 5 km is necessary for the determination of the PMC geographic location and GW horizontal scale-sizes for detailed orbit-to-orbit spatial/temporal investigations. These limits are well within those needed for modeling the effects of the GW on PMC formation using existing models and will be sufficient for much higher resolution (nested-grid-type) modeling of PMC formation using the combined AIM data set.

Altitude Range: 81-85 km
Horizontal Resolution: 3 km in nadir
Vertical Resolution: 3 km
Temporal Resolution: Individual Measurement: 0.4 sec.
Measurement Rate: 1 image set per 60 sec.
Precision: ±5 km in nadir

5.2.2 Temperature

Once the PMC morphology is established, frost point conditions will be inferred using the measurements of H_2O (or OH) abundance and temperature. PMC will be sorted to select air parcels that are so highly supersaturated that GW effects will not have unsaturated the air and sublimated the PMC in the recent past. Such an approach unambiguously determines how the availability of nucleation sites plays a role in the observed PMC morphology.

The temporal resolution required to calculate the degree of H_2O saturation in the summer polar mesosphere needs to be higher than previous work which described the seasonal variation of temperature in 1 week increments [Lübken, 1999]. Clear air measurements can be co-averaged and then compared against air parcels containing PMCs on a daily basis to satisfy the science objective. We expect that the lowest temperature observed in the summer polar mesosphere will be ~128 K with gravity wave variability about this of ±10 K [Lübken, 1999; Lübken and von Zahn, 1991]. Since saturation conditions are typically reached at ~150 K for ambient water vapor at 82 km, AIM needs to sort over a significant fraction of unambiguously supersaturated air so an accuracy of ±5 K is needed.

Altitude Range: 81-85 km
Vertical Resolution: 3 km
Horizontal Resolution: 500 km
Temporal Resolution: 1 day
Accuracy: ±5 K

5.2.3 Water Vapor

The H_2O mixing ratio has a relatively small impact on the calculation of saturation conditions compared to temperature so that a 50% uncertainty in mixing ratio will satisfy the minimum science here. The horizontal resolution for temperature and H_2O must be at least as good as the state-of-the-art GCM models, which is 5° in latitude or about 500 km [Roble and Ridley, 1994].

Altitude Range: 81-85 km
Vertical Resolution: 3 km
Horizontal Resolution: 500 km
Temporal Resolution: 1 day
Precision: 50%

5.2.4 Summary of Geophysical Parameters Required for Objective 2

	PMC Morphology		Temperature		Water Vapor	
	Min	Goal	Min	Goal	Min	Goal
Altitude Range (km)	81-85	75-95	81-85	75-95	81-85	75-95
Vertical Resolution (km)	3	1	3	1	3	1
Horizontal Resolution (km)	3	2	500	150	500	150
Temporal Resolution	0.4 sec	0.2 sec	1 day	1 min	1 day	1 min
Precision	±5 km	±2 km	±5 K	±1 K	50%	10%

6 Objective 3. Temperature Variability

6.1 Science Question

How does dynamical variability control the length of the cold summer mesopause season, its latitudinal extent and possible interhemispheric asymmetry?

Given that PMCs are likely indicators of extremely low temperatures and thus of dynamically induced departures from radiative equilibrium, it follows that to understand why PMCs form, we must understand the dynamical factors controlling the existence of the cold summer mesopause. AIM will measure the temperature and dynamical quantities, gravity wave activity and the mean upwelling, which govern the large deviations of the mesopause temperature from radiative equilibrium. *Luo et al.* [1995] suggested that seasonal variations in wave activity are responsible for the abrupt seasonal temperature changes that are observed. The combination of AIM temperature measurements and wave imagery will allow us to test this hypothesis.

Concerning the upwelling rate, *Gadsden* [1999] has recently suggested that there is a distinct outer edge (i.e. low latitude boundary) to this upwelling and that changes in the latitude of this edge could help define long-term trends. AIM will measure key tracers that exhibit vertical gradients at different altitudes thus allowing vertical winds (mean upwelling rate) to be inferred. This has been done in the stratosphere using UARS data (e.g. *Strahan et al.*, 1996). AIM CH_4 data will be used in the upper stratosphere and lower mesosphere and H_2O in the middle mesosphere. Temperature measurements will allow the gradient wind to be constrained derived [*Lieberman*, 1999]. Thus these tracers and temperature data gradient winds will constrain 2D and 3D global models of the mesospheric residual circulation.

Finally, the relative weakness of MST radar echoes (PMSE) in the SH has led some to assert that the southern summer is 5-10K warmer than the Northern summer [*Huaman and Balsley*, 1999.], although While this result is controversial [e.g. *Lübken et al.*, 1999, recent 2D global modeling has reproduced a similar hemispheric temperature asymmetry [*Siskind et al.*, 2003]. If true, this will have important implications for the relative brightness of PMCs between the NH and SH. Indeed, there is evidence of brighter PMC in the NH [*Thomas and Olivero*, 1989]. The AIM temperature measurements will resolve this question directly. Using AIM data results we will also look for possible N/S differences in gravity wave activity and upwelling rates which might affect variations in PMC brightness.

6.2 Required Geophysical Parameters

Here, "temperature variability" is meant to cover the broad seasonal scales of temperature variability in the summer polar mesosphere produced by large-scale dynamics, radiation and photochemistry. Thus, the "temperature variability" assessed here applies only to answering AIM-related science questions targeted to those particular large scales of motion. In particular, it must be stressed that "temperature variability" is not covered solely under Objective 3 – indeed, temperature data are vital to most of the other science objectives, and in some cases the requirements on the temperature measurements from those objectives generally differ from those to be outlined here.

The requirements here depend most obviously on the direct temperature measurements, which are addressed first and in greatest detail. Coincident PMC brightness measurements are invoked to investigate the proposed hemispheric asymmetry of the PMC appearance and their correlation with the large-scale temperature environment. At the end we also address measurements of CH_4 and H_2O mixing ratios, which can be used to infer mean upwelling rates in the polar summer mesosphere, which in turn affect local temperatures.

6.2.1 Temperature

(a) Accuracy. Ground-based measurements of summer polar mesosphere temperatures are very sparse, since most optical mesospheric temperature sensors cannot operate in perpetual daylight conditions. Daytime measurements of polar mesospheric temperatures by powerful new Rayleigh and sodium (Na) lidar systems are being planned [*Rees et al.*, 2000]. Initial daytime Na lidar measurements at mid-latitudes in summer produced temperature profiles with uncertainties in the range ~5-20 K at ~80-90 km for 1 hour integrations [*States and Gardner*, 2000]. Thus rockets, and particularly falling spheres (see Figure 3.1), remain one of the more important data sources. Uncertainties in temperatures from the latest falling sphere experiments are ~7 K at 90 km and ~3 K at 80 km [*Schmidlin et al.*, 1991], implying uncertainties of ~4-5 K at PMC altitudes. The falling sphere data are also insensitive to small vertical scales: at PMC altitudes, structures with vertical wavelengths < 8 km or so are not resolved [*Lübken et al.*, 1999], implying an effective vertical resolution of ~4 km. Of existing satellite temperature measurements at PMC altitudes, data from the HRDI instrument on UARS appear to be the best at present [*Huaman and Balsley*, 1999]. While a complete error analysis of HRDI temperatures is not available, *Huaman and Balsley* [1999] quote an estimated uncertainty of ~7 K at summer mesopause altitudes.

Thus, a 5K measurement accuracy in temperature measurements matches or improves upon the best available measurements from this region. Given typical temperatures of ~130-7160 K at PMC altitudes (see Figures 3.1 and 3.3), +/- 5 K implies a net uncertainty of ~3%, with a goal of attaining twice the accuracy than has heretofore been obtained from this region (+/- 2 K). This degree of accuracy is well below the typical geophysical temperature variability that occurs at these altitudes due to the effects of planetary waves and gravity waves [*Avery et al.*, 1989; *Williams and Avery*, 1992; *Gerrard et al.*, 1998; *Lübken*, 1999; see Figures 3.1 and 3.2; see also Objective 2], and also allows us to identify all the major seasonal and hemispheric variations of relevance to PMC evolution (see below).

Temperature Accuracy: Minimum 5 K (3%), Goal 2 K (1%)

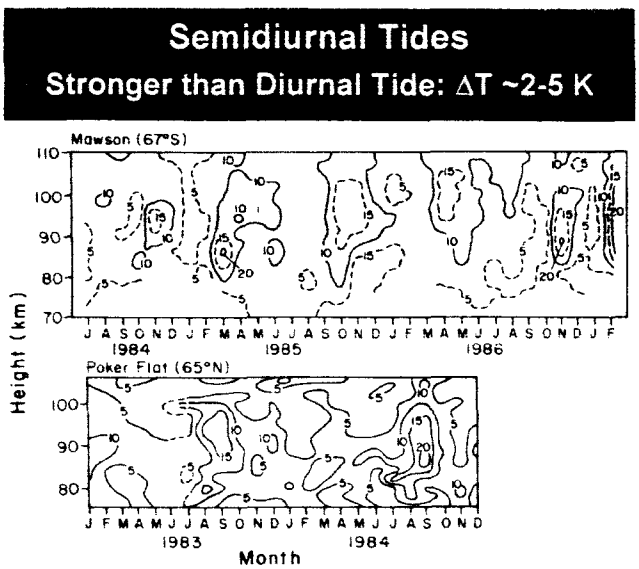

Figure 3.2: Height-season variations of semidiurnal tide horizontal wind amplitudes (in m s^{-1}) measured by radars at Poker Flat, Alaska (65°N) and Mawson, Antarctica (67°N) during years 1983-1986 [after *Avery et al.*, 1989]. These values translate to temperature amplitudes of ~2-5 K, according to tidal theories.

(b) Precision. Although mesospheric temperatures are geophysically variable, atmospheric dynamics, radiation, photochemistry and PMC microphysics are all acutely dependent on the absolute value of temperature. Experience in the polar stratospheric cloud (PSC) community suggests that knowledge of large-scale and mesoscale temperatures to a systematic uncertainty of less than 1-2 K (~0.5-1%) can sometimes be necessary to adequately model the microphysical evolution of PSCs [e.g., *Pawson et al.*, 1999]. Similar temperature thresholds for the PMC environment may ultimately be required. A total accuracy of 5K (minimum) and 1K (goal) therefore yields a precision of slightly less than 5K $[(5K)^2-(1K)^2]^{1/2}$, minimum) and <2K ($[(2K)^2-(1K)^2]^{1/2}$, goal).

Temperature Precision: Minimum <5K (<3%), Goal <2K (<1%)

(c) Vertical Resolution. As discussed above in (a), falling sphere data (our best current observational source on summer mesospheric temperature variability) have an 8 km minimum vertical scale resolution, which implies an effective vertical resolution of ~4 km. Thus, we impose a similar 4 km minimum vertical resolution requirement for AIM temperatures, to meet our criterion of acquiring temperature profiles from this region to an accuracy and resolution equal to or better than has been achieved before. We set a goal of nearer 2 km, as this resolves the vertical wavelengths of all the major planetary waves and gravity waves at these altitudes, which all generally have wavelengths > 5 km. This also allows us to separate potentially important altitude regions associated with the mesopause, PMC layers, PMSE layers, and various water layers.

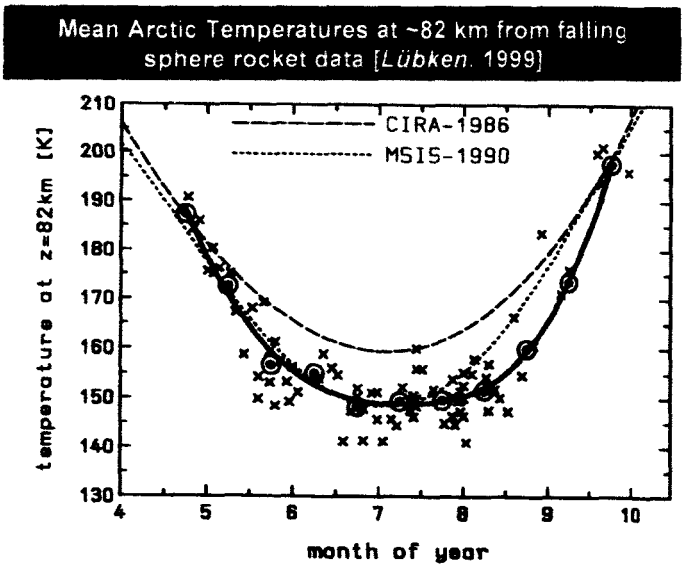

Figure 3.3: Seasonal variation of mean Arctic temperatures at ~82 km from instantaneous falling sphere data (crosses), weekly averages (circles), and a smoothed spline fit (solid line). Estimates from CIRA and MSIS empirical models are shown with broken lines. Note the rapid 5-10K/week cooling and warming at the start and end, respectively, of the PMC season [after *Lübken*, 1999].

Temperature Vertical Resolution: Minimum 4 km, Goal 2 km

(d) Temporal Resolution. Figure 3.3 shows the seasonal variation of Arctic falling sphere temperatures at a nominal PMC altitude of ~82 km [*Lübken*, 1999]. The data show that mean temperatures (solid curve) stay relatively constant at ~153 +/ 3 K from early June through to mid August, a period during which NLCs are frequently observed from the ground [*Lübken*, 1999]. Before June and after mid-August, mean temperatures decrease and increase, respectively, by ~5-10 K per week, corresponding to a rapid increase and decrease, respectively, in NLC occurrences [*Lübken*, 1999] (the rapid shift between warm wintertime conditions and cold summertime conditions was first observed by *von Zahn et al.* [1996] using ship-based lidar). AIM temperature data must be able to distinguish these temperature transitions associated with the start and end of the PMC season. Temperature differences of 5K are above the accuracy/precision minima of the temperature data described above. Attaining this 5 K global temperature discrimination at a temporal resolution of 74 days is considered a minimum mission requirement to resolve these seasonal trends. As a goal, 5 K uncertainties in global temperatures acquired each day will pin down the precise space-time transitions to/from PMC seasons in unprecedented daily detail. Such discrimination also allows day-to-day investigations of possible interhemispheric differences in mid-summer polar mesosphere temperatures of ~5-10 K (see Figure 3.4) that may explain less intense PMSE and PMC brightnesses in the Southern Hemisphere [*Thomas and Olivero.*, 1989; *Huaman and Balsley*, 1999; *Woodman et al.*, 1999; *Carbary et al.*, 2001]. Daily resolution here need not be attained with full hemispheric y global coverage, given that zonal asymmetries in temperature are not expected to be very large in the summer polar mesosphere.

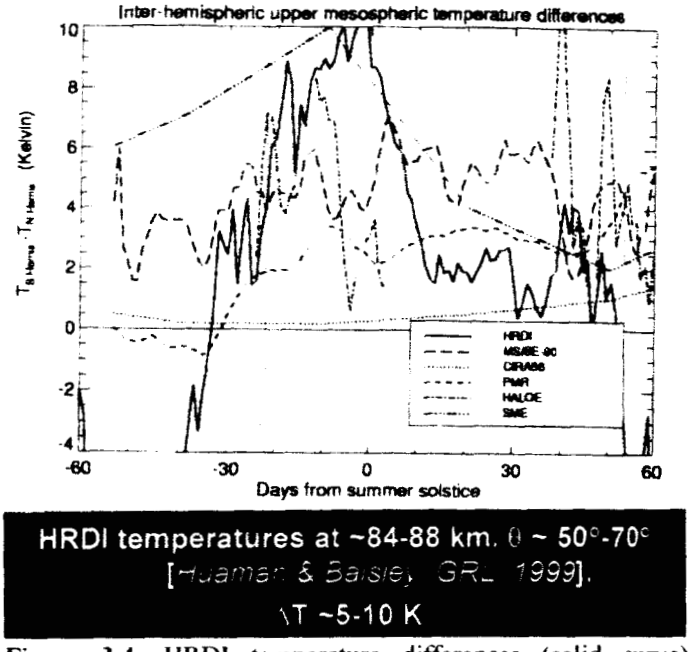

Figure 3.4: HRDI temperature differences (solid curve) between the southern and northern hemisphere in the 50°-70° latitude band, plotted as a function of days from summer solstice. Data from other sources are also shown: see *Huaman and Balsley* [1999] for full details. Differences ~5-10 K are evident, suggesting a warmer summer polar mesosphere in the southern hemisphere.

Individual temperature profiles can be acquired with greater accuracy by using longer integration times, at the expense of the final spatial and temporal resolution of the data along the orbital track. Given the likely structure and variability in PMC images [see, e.g., *Carbary et al.*, 2000; *Gadsden*, 2000], we will acquire temperature data with as much spatial and temporal resolution as possible in the temperature data to aid interpretation of these structures. This implies short integration times where possible. While such data necessarily have greater intrinsic measurement uncertainties, subsequent averaging of data points over successive orbits or over synoptic regions of the polar cap can yield temperature estimates with smaller uncertainties where necessary. For individual data with a 5 K statistical (nonsystematic) uncertainty, averaging of 5100 data points, closely spaced either geographically or in time, yields a mean with an uncertainty of ~1.30.5 K. Such methods are used routinely in ground-based data and prove entirely adequate for detecting long-term temperature trends, for example [e.g., *Keckhut et al.*, 1995].

Temperature Temporal Resolution: Minimum 4 days, Goal 1 day

(e) Horizontal Resolution. Final spatial resolution of the limb-scanned temperature data is controlled by the intrinsic sensitivity of the instruments, scan rates and the orbital geometry. Previous observations with limb-scanning IR, microwave and UV instruments indicate that limb-scanned temperature data can resolve structures with horizontal scales >50-200 km and vertical scales >5-15 km, with the limits varying from instrument to instrument [*Fezter and Gille*, 1994; *Wu and Waters*, 1997; *Preusse et al.*, 2000; *McLandress et al.*, 2000]. Faster scan rates yield a better resolution of short spatial structures in the limb-scanned temperatures, particularly along the orbital track. This also yields a greater number of data points per scan, and better synoptic data coverage. Accumulated observations and models suggest perturbations of ~2-5 K at PMC altitudes from tides, and 2-day, 5-day and 16-day planetary waves [*Williams and Avery*, 1992; *Avery et al.*, 1989; see Figure 3.2], with complex nonlinear interactions among them [e.g., *Forbes et al.*, 1995] and potential space-time aliasing issues for tides in the AIM sampling [e.g., *Azeem et al.*, 2000].

To resolve and unravel all these processes, model studies suggest that, at a minimum, we need to resolve apparent planetary wavenumbers up to zonal wavenumber 4 [see, e.g., *Fetzer and Gille*, 1994; *Palo et al.*, 1999]. This resolves the dominant migrating tides (wavenumbers 1-2) as well as possible 2 day, 5 day and 16 day waves (wavenumbers 1-4). Latitudinal resolution helps us to resolve the latitudinal Hough mode structures of the various modes as well. Note in particular that PMC maps from SNOE have revealed clear planetary wave structures out to wavenumber 3 [*Thomas, private communication*, 2000]. These factors combine to give us a necessary minimum longitudinal-latitudinal resolution of

45°x5° for the temperature data (i.e., 12x8 points over the hemisphere poleward of 60-65°N, corresponding to ~1700x500 km resolution near 70°N).

Where latitudinal coverage cannot be achieved, we will use available ground-based data to supplement the observations as well as 2D and 3D atmospheric models constrained by AIM data (see section 3.1) to simulate the evolution of the hemispheric polar summer mesopause temperatures. For example, powerful new daytime lidar systems operating at select high northern and southern latitude sites will be available to provide correlative and supplementary temperature data. Assimilative global modeling is a well accepted method of combining available observations to attain a best estimate of the global state of the atmosphere [e.g., *Akmaev*, 1999]. With the use of such models, the required horizontal resolution can be achieved with 45° longitudinal resolution at a single latitude. Our goal is to detect leakage of power of migrating tides into higher zonal wavenumbers (5, 6) due to nonlinearity and/or wave-wave coupling. Pushing the sampling to 5°x2° resolution would allow an analysis at the standard resolution of National Centers for Environmental Prediction (NCEP) tropospheric and stratospheric analyses, which capture all major synoptic scale weather events. Similar resolution at PMC altitudes will provide unprecedented detail on the synoptic meteorology of the polar summer mesosphere. An important point here is that existing global mesosphere-thermosphere models, such as the TIME GCM, currently initialize their simulations using NCEP geopotential height fields at some stratospheric lower boundary level. Given advances in computing capabilities, we expect these and other new models (e.g., NRL's High-AltitudeSkyHigh NOGAPS model – *Coy et al.*, 2002) to be operating at longitude-latitude resolutions as good or even better than the current 5°x2° set by these standard NCEP analysis fields. Striving for this extra resolution where possible will allow us to conduct comparisons with global model simulations at an unprecedented level of spatial detail.

Temperature Horizontal Resolution: Minimum 45°longitudinal resolution, Goal 5°x2° (lon x lat)

6.2.2 PMC Brightness

PMC brightness measurements with the *same horizontal, vertical and temporal resolution as the temperature measurements* are required to investigate the influence of the large scale temperature environment on the PMC appearance, especially the reported asymmetry in PMC brightness between the summer hemispheres. The brightness data reported by *Thomas and Olivero* [1989] suggest that an accuracy of 50% together with a precision of 20% is sufficient to fully address this issue. Brightness measurements of higher quality (10% accuracy and 5% precision) would allow an even more detailed investigation of the large large-scale dependencies of cloud brightness on quantities like temperature, gravity wave activity, nucleation sites, and water vapor, and is thus considered to be a goal. Such PMC brightness data will provide our fundamental measurement of PMCs for correlation with temperature data: e.g., the duration of the PMC season for comparison with seasonal variations in mesopause temperatures as set forth in section 3.2.1(d).

To study the overall influences of gravity wave-related temperature variability on PMCs, much more stringent requirements on PMC brightness measurements are necessary in order to extract information on the gravity wave environment from these measurements. These requirements are identical to the ones that are necessary to address Objective 2.

6.2.3 *CH_4 and H_2O mixing ratio profiles*

Synoptic temperature data with the baseline characteristics outlined above provide a powerful constraint on the global dynamics of the mesosphere, particularly mean meridional and vertical winds, which drive the atmosphere here well away from radiative equilibrium. Global mesospheric temperature data can also be used to effectively constrain derived mesospheric wind patterns quite accurately [*Lieberman*, 1999; *Frame et al.*, 2000; *Oberheide et al.*, 2000]. Better space-time resolution and accuracy in global temperature measurements yield better final wind estimates, given the dependence of these calculations on temperature gradient terms.

AIM will also measure trace chemicals that, at certain altitudes, have long enough chemical lifetimes that they approximate tracers of the atmospheric motion. Examples include methane (CH_4) in the upper stratosphere and lower mesosphere and water vapor (H_2O) in the middle mesosphere. Fully interactive 2D and 3D global model simulations using these observations can be used to pin down accurately the residual circulation as well as vertical and lateral mixing, which help to better constrain 2D and 3D models of the mesospheric residual circulation [e.g., *Siskind et al.*, 2003].

To achieve this, we require measurements of these chemical abundances that have similar (or slightly coarser) spatial and temporal sampling characteristics to the temperature data quoted above. As regards accuracy and precision, the key factor here is the absolute accuracy/precision of the final mixing ratio estimates, since mixing ratio (rather than number density) is the critical measure when using these trace constituents as tracers of the motion [e.g., *Eckermann et al.*, 1998]. Based on previous work for both water and methane [e.g., *Summers et al.*, 1997], an ability to distinguish differences of ~1 ppmv in these profiles will be more than sufficient to enable us to model the way in which their mixing ratio gradients are advected and mixed both vertically and latitudinally in the summer polar mesosphere. We define this mixing ratio threshold as our minimum accuracy, with a goal of twice this minimum sensitivity (i.e. 0.5 ppmv). Precision here is less of a concern, since it is only mixing ratio *gradients* that are important for gleaning mean vertical and meridional transport, as well as for locating regions where gradients have been largely removed by strong meridional and/or vertical mixing. Thus, we impose similar requirements on precision as we do for accuracy.

Mixing Ratio Resolutions: Basically Similar or Slightly Less Stringent Than Those for Temperature
Mixing Ratio Accuracy: Minimum 1ppmv, Goal 0.5 ppmv
Mixing Ratio Precision: Minimum <1ppmv, Goal <0.5 ppmv

6.2.4 *Summary of Geophysical Parameters required for Objective 3*

	PMC Brightness (limb scanned)		PMC Brightness (nadir)		CH_4 Mixing Ratio		H_2O Mixing Ratio		Temperature	
	Min	Goal	Min	Goal	Min	Goal	Min	Goal	Min	Goal
Vertical Resolution (km)	4	2	N/A	N/A	4	2	4	2	4	2
Horizontal Resolution (lon×lat)	45°×5°	5°×2°	3 km	2 km	45°	10°×2°	45°	10°×2°	45°	5°×2°
Temporal Resolution	74 days	1 day	0.4 sec	0.2 sec	1 week	1 day	1 week	1 day	74 days	1 day
Accuracy	50%	10%	15%	15%	1 ppmv	0.5 ppmv	1 ppmv	0.5 ppmv	± 5K	± 2K
Precision	20%	5%	5%	5%	1 ppmv	0.5 ppmv	1 ppmv	0.5 ppmv	± 5K	± 2K

7 Objective 4. Hydrogen Chemistry

7.1 Science Question

What are the relative roles of gas phase chemistry, surface chemistry, dynamics and condensation /sublimation in determining the abundance and variability of water vapor in the polar mesosphere?

Despite the key role that water (vapor and ice) plays in the formation and evolution of PMC's, direct measurements of the water abundance along with PMC properties in the PMC formation region of the polar mesosphere are relatively rare. However, there are several distinct processes which probably influence the abundance of and variability of water in the region of the polar mesosphere where PMCs have been observed. Since PMCs are composed of water ice, understanding the processes which control water vapor in the summer polar mesosphere will provide a basis for understanding the formation and evolution of PMCs themselves.

Water vapor is transported upward into the meososphere from the lower atmosphere by both advective and diffusive processes. Water vapor is also produced by the photochemical destruction of CH_4 that occurs primarily in the stratosphere. In addition, gas phase chemistry can contribute to both production and loss of water vapor. H_2O is the source molecule for odd hydrogen radicals ($H + OH + HO_2 = HO_x$) that catalytically destroy mesospheric odd oxygen ($O + O_3 = O_x$) (Brasseur and Solomon, 1986). This chemistry also contains chemical pathways for the production of water vapor from hydrogen radicals. There is also indirect evidence that heterogeneous chemistry on meteoric dust particles releases water vapor locally in the mesosphere, which provides a kinetic mechanism for conversion of chemical stable H_2 back into H_2O. All of these processes, in addition to phase changes of water, probably contribute to controlling the water vapor abundance in the polar mesospheric cloud formation region. Thus understanding hydrogen chemistry must be done within the context of understanding the relative roles of these various processes.

In this section we ask the following two questions:

1) What is the water vapor distribution (and its variability), and how accurately (spatial and temporal resolution) do we need to know its distribution in order to understand what controls it?

2) What additional measurements besides water vapor are required in order to separate the roles of gas phase chemistry, surface chemistry, and transport in controlling the abundance and variability of mesospheric water vapor.

We will begin by considering polar mesospheric water vapor in the absence of PMCs and then discuss the complexities added by the existence of PMCs.

7.2 Required Geophysical Parameters

7.2.1 Trace gases and temperature to investigate hydrogen chemistry in the absence of PMCs.

It is important to understand gas phase odd-hydrogen chemistry because it determines the gas phase production and loss of H_2O.

The water vapor distribution in the mesosphere has been studied extensively, and its gas phase chemistry is thought to be relatively easy to quantify, at least in principal. Both water vapor and CH_4 enter the low latitude stratosphere at the tropopause and are advected upward by the residual circulation. During its ascent CH_4 is oxidized to H_2O primarily in the stratosphere. The peak in H_2O generally occurs near ~50-60 km altitude. Chemical destruction of H_2O above that altitude (by solar photolysis and reaction with $O(^1D)$) leads to, in general, a decreasing mixing ratio with altitude. Polar transport

also occurs due to meridional advection in the mesosphere. Near the poles this picture is modified by the residual circulation, which is downward in winter and upward in summer, and leads to a vertical shifting and compression/expansion of the middle atmospheric water vapor mixing ratio distribution. At high latitudes horizontal mixing can also play a role in pole-ward transport of H_2O (Brasseur and Solomon, 1986).

The characteristic length scale over which mesospheric H_2O varies is determined by the competition between transport (timescale ~ weeks to months) and chemistry (also weeks to months). In the winter polar mesosphere (no PMCs) the vertical scale height for H_2O is approximately 6 km (above 75km) or larger (50-75km). During the summer the vertical scale is somewhat larger. The horizontal scale is a bit more difficult to quantify but HALOE observations show that horizontal variations of approximately 1 ppmv can occur over 10 degrees of latitude (Summers et al., 1997). Similar numbers apply to CH_4 below approximately 65km. From this we suggest that observations of H_2O and CH_4 with a minimum vertical resolution of 3 km (2km goal) between 50-85 km altitude and 20 degrees (15 deg goal) horizontal resolution can adequately characterize the large scale H_2O and CH_4 spatial distributions in the polar mesosphere and thus the large scale source of H_2O to the PMC regions between 80-85 km. From these planned measurements it will be possible to utilize 3-dimensional chemical-dynamical models, anchored by these observations, to build up a 3-dimensional picture of the polar atmospheric H_2O and CH_4 environment. Both H_2O and CH_4 will also be used as tracers of dynamical processes (diffusion and advection), along with gravity wave observations (vertical mixing), the CO_2 distribution, and temperature, to constrain the dynamical model.

Observational Requirements to quantify, i.e. map, CH_4 and H_2O in mesosphere and upper stratosphere:

- *This will provide tracers of transport processes*
- *This will also provide large scale source of H_2O and CH_4 → H_2O conversion*

Vertical resolution: 2 km (3 km min)
Horizontal resolution: 15° (20° min)
Temporal resolution: 1.5 hrs (2 hours min)
Accuracy: 10% (20% min)
Precision: 5% (10% min)

In order to validate odd-hydrogen chemistry in order to quantify the local gas phase production and loss of water vapor is it necessary to have coincident observations of H_2O, O_3, and temperature. The procedure to do this involves using a local (1D) photochemical model (Summers et al., 1996; 1997; 2000). This model will be utilized with fixed (observed) values of H_2O and T to simulate the local diurnal variation of O_3, thus providing a critical test of whether currently formulated HOx and Ox chemistry is complete or needs "tuning" as suggested by many previous studies. Observations of T are required because some key chemical kinetic rate coefficients are temperature dependent. The need to test local HOx chemistry over a range of longitudes and throughout the year is to determine whether the observed O_3 shows the dependence upon H_2O, O_3, and T as expected by photochemical theory (DeMore et al., 1997).

Do we understand H_2O chemical prod/loss and HOx chemistry well enough to do this? Under conditions where the H_2O chemical lifetime is long and not determined by surface chemistry and/or sublimation/condensation, standard photochemical theory leads to an O_3 dependence on H_2O to a power of between 0.5 –1.0 (Allen et al., 1984). To the extent that it is not will indicate inadequacies in our understanding of HOx chemistry. From this perspective, observations of H_2O, O_3 and T before and after the PMC season may be the most important for validating HOx and associated Ox chemistry.

What are the measurement requirements for testing HOx chemistry outside the PMC season? From our previous experience with MAHRSI OH and HALEO H_2O observations (Conway et al., 1996;

Summers et al., 1996) a vertical resolution of 2 km (H_2O, O_3 and T) seems adequate for model/data HOx studies (however, see Complication 1 below).

Observational Requirements to validate HOx chemistry with coincident H_2O, O_3 and T:
- *This will provide means to quantify gas phase H_2O production and loss*

Vertical resolution: 2 km (3 km min)
Horizontal resolution: 15° (20° min)
Temporal resolution: 1.5 hr (2 hr min)
Accuracy: 10% (20% min)
Precision: 5% (10% min)

7.2.2 Trace gases and temperature to investigate heterogeneous chemistry in H_2O layer(s) below PMCs

It is important to understand the source of H_2O in lower layer (65-75 km) because the layer may be causally connected to H_2O in the PMC layer. Also, understanding the source of this layer will give us constraints on the role of heterogeneous chemistry in the mesosphere.

There is considerable evidence that gas phase chemistry alone cannot explain the entire distribution of H_2O in the mesosphere. Support for this comes from our previous work of the MAHRSI OH data along with HALOE H_2O data (Russell et al., 1993), that confirmed the existence of a narrow low latitude layer (~65-70 km) of mesospheric H_2O that cannot be explained by conventional gas phase chemistry (Summers et al., 1997; Siskind and Summers, 1998). It has been proposed that O and H_2 recombine on meteoric dust particles to produce H_2O vapor as a source of this low latitude H_2O layer (Summers and Siskind, 1999).

Recently, we have used high latitude OH data to infer H_2O. Analysis of MAHRSI OH (August, 1997) and HALOE H_2O (June, July and August, 1997) observations suggests that there are one or more H_2O layers below the PMC region during the PMC season (see e.g., Fig1-3a in AIM proposal) (Summers et al., 2001). In the MARHSI OH data this lower H_2O is indicated by a localized OH enhancement peaking near 70 km altitude and seen in almost all MAHRSI OH limb scans. HALOE H_2O data in the same atmospheric regions have been recently re-analyzed using differential absorption between IR channels to remove PMC particle extinction. The HALOE H_2O data were daily averaged to beat down the noise, and indicated the definite presence of 1 and possibly 2 layers in the same altitude region, but there is still some difficulty knowing whether residual noise is present. Zonal plots of the HALOE H_2O data suggest that the high latitude lower altitude layer may be a morphological extension of one observed at lower latitudes (Summers et al., 1997). If so then it may be produced by the same mechanism. In order to make progress understanding the source of this lower altitude H_2O layer, we will require more than the above isolated snapshots of polar mesospheric H_2O, at higher vertical resolution than are unobtainable from current ground based techniques for measuring H_2O [Nedoluha et al., 1999]. This is essential given the layering that appears to be present.

Given the higher mesospheric temperatures at lower latitudes, and at high latitudes below the PMC region, it is implausible that these layers are due to water vapor condensation/sublimation physics (Thomas, 1991). Since the observed lower layer does not appear to be morphologically connected to the PMC region near 82 km, it may be that they are due to completely independent mechanisms. Is it possible that there is a causal connection between the lower layer and PMCs? It may be that the lower layer preconditions the formation of PMCs at the higher altitude because elevated H_2O abundances lofted into the ~82 km region will increase the relative humidity early in the PMC season.

Is it possible that the mechanism that produces the lower layer somehow affects HOx chemistry? That is unlikely because1) the H_2O lifetime is of order several weeks at the location of the lower layer, whereas the lifetime of OH and HO_2 is of order a minute, 2) the enhancement of H_2O seen in the lower layer is only of order 10-20% of the background H_2O abundance, and 3) the collision rate of OH and HO_2 to the surface sites that could serve to catalize surface H_2O production within the layer is of order 1% of the HOx catalytic cycling time. In order to pursue these questions we will need to follow the formation/evolution of the lower layer for a long period of time, which we will accomplish by the SOFIE measurements.

The HALOE H_2O measurements appear to resolve the vertical structure of this lower layer, thus a comparable vertical resolution of 3 km (2 km goal) will be required. In terms of temporal variation of this layer from the HALOE observations it appears to respond to changing meridional circulation in a similar manner as the background water distribution and may thus have a comparable chemical lifetime (order weeks or longer). If the layer is due to heterogeneous chemistry as we've previously suggested then the chemical time scale is of order 2 weeks.

Observational Requirements to spatially resolve O_3, H_2O and T in lower water vapor layer:

- *This will allow us to determine relative surface/gas source of H_2O*
- *This will allow us to determine if elevated H_2O causally connects to PMC layer*
- *Provide means to determine if surface chemistry affects HOx*

Vertical resolution: 2 km (3 km min)
Horizontal resolution: 15° (20° min)
Temporal resolution: 90 min (2 hr min)
Accuracy: 10% (20% min)
Precision: 5% (10% min)

7.2.3 Trace gases to investigate the hydrogen chemistry in and above the PMC region.

Gas phase hydrogen chemistry in the PMC region acts as both a sink and minor source of H_2O vapor.

Our studies of H_2O from both the MAHRSI OH and HALOE H_2O data within the PMC formation region is that very large H_2O mixing ratios are present *whether or not PMCs are present* (as evidenced in enhanced solar backscatter radiation in the MAHRSI OH observations and as enhanced solar IR extinction in the HALOE measurements). This narrow layer (see e.g., Fig1-3a in AIM proposal), centered between 82-84 km altitude, exhibits water vapor mixing ratios ranging from 10 to over 15 ppmv and considerable spatial variation. This implies that PMCs are very efficient at dehydrating air flowing vertically through them and thus very effective at sequestering total water (both ice and vapor) within the layer. There are several considerations regarding measurements needed to study hydrogen chemistry within the PMC region that we will address here.

From Fig1-3a it is seen that the observed OH enhancement near 82 km leads to very sharply peaked inferred H_2O that is not resolved in the OH data nor in the model. Individual MAHRSI scans with much larger values of retrieved OH (and higher H_2O mixing ratios) appear similar. Part of the sharply peaked H_2O inferred from the observed OH is due to the current model vertical resolution of 2km between grid points. A higher vertical resolution photochemical model will need to be developed and our current estimate is that the model vertical grid spacing smaller than .5km will be necessary to resolve the (inferred) H_2O profile within the PMC layer. The major uncertainty here is that we really don't know just how sharply peaked the actual H_2O layer is. From the topside MAHRSI OH measurements we find that the OH typically falls off by a factor of 5 between about 83 and 86 km and the inferred H_2O decreases by a factor of 9. This implies that the H_2O scale height is less than 1.5 km above the peak

H_2O. But it could be smaller. In order to determine the amount of dehydration of the air flowing upward thru the PMC layer it is important to characterize this topside behavior. It may not be essential to actually resolve the H_2O layer in order to determine the total gas phase H_2O production and loss, and that may be accomplished by knowing the H_2O "column" within the layer. The photochemical model may then determine the gas phase H_2O production and loss within that PMC "column."

Another key question regards the contribution of surface chemistry to the water vapor budget within the PMC region. Observations of PMCs and O by Gumbel (1999) suggest that O is depleted in the presence of clouds; however, the chemical implications of such depletions for water vapor are not clear. Simultaneous measurements of H_2O and O_3 will be required to allow for a rigorous test of our understanding of HO_x/O_x chemistry in this region. By studying the chemical relationships between H_2O and O_3 under conditions with and without PMCs, the role of heterogeneous chemistry may possibly be statistically isolated, (e.g. Summers and Siskind, 1999; Thomas, 1991).

7.2.4 Summary of Geophysical Requirements for Objective 4:

	H_2O, CH_4		O_3		Temperature	
	Min	Goal	Min	Goal	Min	Goal
Altitude Range (km)						
Vertical Resolution (km)	3	2	3	2	3	2
Horizontal Resolution (lon)	15°	20°	15°	20°	15°	20°
Temporal Resolution	2 hour	1.5 hour	2 hour	1.5 hour	2 hour	1.5 hour
Accuracy	20%	10%	20%	10%	5K	
Precision	10%	5%	10%	5%	3%	

8 Objective 5. PMC Nucleation Environment

8.1 Science Question

Is PMC formation controlled solely by changes in the frost point or do extraterrestrial forcings such as cosmic dust influx or ionization sources play a role?

As with tropospheric clouds, mesospheric ice particles should form when mesospheric H_2O becomes super-saturated, but only if there are suitable nucleation sites available on which the water vapor may condense. For PMCs, it is unknown which of these conditions is the rate-limiting step controlling their temporal variability. Cosmic dust is thought to serve as a primary nucleation site for PMCs [Hunten et al., 1980]. In addition to the AIM frost point data, we will provide a simultaneous determination of the incoming flux of cosmic dust. Dust particles travel in about 1 minute from the satellite altitude of 550 km to the upper mesosphere where they ablate and re-condense as "smoke" particles. AIM in-situ measurements of the incoming dust flux will be used in conjunction with microphysical models of dust ablation and coagulation to deduce the average number of condensation nuclei available in the mesosphere through this process. Modeled profiles of meteoric smoke size distributions were recently used to simulate the SOFIE response. These results indicate that smoke extinctions could be a factor of 10 above the SOFIE noise floor and thus readily detected. Combining these measurements with the incoming dust flux will provide a more complete understanding of meteoric particles and their role in PMC microphysics. We will correlate large changes in the dust influx with possible changes in the occurrence rate and brightness of the PMCs for cases of nearly identical frost-point conditions.

A second possible nucleation site is proton hydrate ions [Witt, 1969]. Reid [1989] has suggested that increased ionization will decrease the heavy proton-hydrate ion density through increased recombination and thus decrease PMC formation. We will use observations of the nitric oxide (NO) abundance as a proxy for the ionization rate [Siskind et al., 1989] and correlate this quantity against PMC morphology for air parcels under similar frost-point conditions. NOAA/TIROS electron flux data [Codrescu et al., 1997] will be used to extend this correlation to locations where we will not have NO data (NO will be measured solely by solar occultation at specific latitudes), but still have cloud and frost point data. An anti-correlation between the inferred ionization rate and PMC brightness will support the Reid [1989] hypothesis. This would have important implications for interpreting long term PMC variability since it is well known that the ionization rate varies roughly with the 11-year solar cycle.

AIM data will not answer all the questions pertaining to the specific mechanism of PMC nucleation. For example, sulfuric acid particles may be a nucleation source but we will not measure H_2SO_4 directly. This mechanism will be considered theoretically, and its contribution to the nucleation processes will be inferred based on conclusions from the dust and ionization investigations. Despite this limitation, we will provide direct tests of published nucleation hypotheses that are relevant for the larger study of mesospheric climate.

8.2 Required Geophysical Parameters

8.2.1 PMC Morphology

In order to attach relevance to the measured PMC nucleation environment, the PMC morphology at any given time must first be defined. This morphology will consist of both (optically active) PMC occurrences and PMC brightness profiles. Since the measurements to be used in the description of the PMC nucleation environment will be made primarily by viewing the limb (e.g. T, H_2O, NO), they implicitly require the assumption of spherical symmetry for their interpretation. Thus an important consideration in establishing the morphology is constraining the PMCs to the tangent height. This can be done by selecting PMC limb scans where the peak in cloud scattering/extinction is at an altitude at which PMCs are known to exist (81-85 km).

To reliably distinguish "clear" from "cloudy" air, it will be necessary to sort data on time scales of ~1 minute at a minimum, during which time the spacecraft travels ~500 km. The vertical resolution should be smaller than this to minimize the amount of smearing as the instruments are viewing nearly in the orbital plane. A 3 km vertical resolution translates to 200 km along the line of sight and will be sufficient.

The contrast in brightness between an observation with a PMC in the line-of-sight and clear air conditions is expected to be large on the limb both in absorption and emission. In establishing the PMC morphology we are only interested in the difference between cloudy and clear air observations. We are also not emphasizing minute differences between the two for this objective. A precision of 56% will suffice here.

Altitude Range: 81-85 km
Vertical Resolution: 3 km
Horizontal Resolution: 500 km
Temporal Resolution: 1 minute @ common volume
Precision: 56%

8.2.2 Temperature

Once the PMC morphology is established, frost point conditions will be inferred using the measurements of H_2O (or OH) abundance and temperature. PMCs will be sorted to select air parcels that are so highly supersaturated that small-scale gravity wave effects will not have unsaturated the air and sublimated the PMC in the recent past. Such an approach unambiguously determines how the availability of nucleation sites plays a role in the observed PMC morphology.

The temporal resolution required to calculate the degree of H_2O saturation in the summer polar mesosphere needs to be higher than previous work which described the seasonal variation of temperature in 1 week increments [Lübken, 1999]. Clear air measurements can be co-averaged and compared against air parcels containing PMCs on a daily basis to satisfy the science objective. We expect that the lowest temperature observed in the summer polar mesosphere will be ~128 K with gravity wave variability about this of ±10 K [Lübken, 1999; Lübken and von Zahn, 1991]. Since saturation conditions are typically reached at ~150 K for ambient water vapor at 82 km, AIM needs to sort over a significant fraction of unambiguously supersaturated air so an accuracy of 5 K is needed.

Altitude Range: 81-85 km
Vertical Resolution: 3 km
Horizontal Resolution: 500 km
Temporal Resolution: 1 day
Accuracy: ±5 K

8.2.3 Water Vapor

The H_2O mixing ratio has a relatively small impact on the calculation of saturation conditions compared to temperature so that a 50% uncertainty in mixing ratio will satisfy the minimum science here. The horizontal resolution for temperature and H_2O must be at least as good as the state-of-the-art GCM models, which is 5 degrees in latitude or about 500 km [Roble and Ridley, 1994].

Altitude Range: 81-85 km
Vertical Resolution: 3 km
Horizontal Resolution: 500 km
Temporal Resolution: 1 day
Precision: 50%

8.2.4 Nitric Oxide

The ability of AIM to determine whether heavy proton hydrate ions are an important nucleation site for PMCs is largely dependent on AIM's ability to infer nitric oxide (NO), which is regarded as a proxy for ionization [Siskind et al., 1989]. NO is readily created by medium energy electrons (MEEs) in the upper mesosphere [Codrescu et al., 1997]. It is therefore important to be able to distinguish the vertical distribution of NO in the upper mesosphere (80-95 km) with that in the lower thermosphere (~105 km). This requires that the vertical resolution be ~5 km or better. This also requires that the temporal resolution be high enough to reliably relate the (sporadic) variation of medium energy electrons with the variations of NO and of PMCs. Based on the lifetime of NO at these altitudes (1-2 days), we choose a temporal resolution of 1 day for minimum science. The horizontal resolution must allow for the auroral oval to be spatially resolved: about 500 km.

The minimum required accuracy and precision of NO between 80-95 km requires an understanding of how NO responds to ionization. Reid [1989] reviewed the topic and found that at 65 N the average electron production rate is about 10 $cm^{-3}s^{-1}$ but during strong disturbances production rates can reach 10^5 $cm^{-3}s^{-1}$. Precipitating MEEs with energies of about 45 keV yield a peak ionization rate at about 84 km for the conditions of the summer polar mesosphere. Figure 5.1 shows the results of a steady-state one-dimensional model calculation of NO using a spectrum of precipitating electrons with a Gaussian distribution and a characteristic energy of 45 keV.

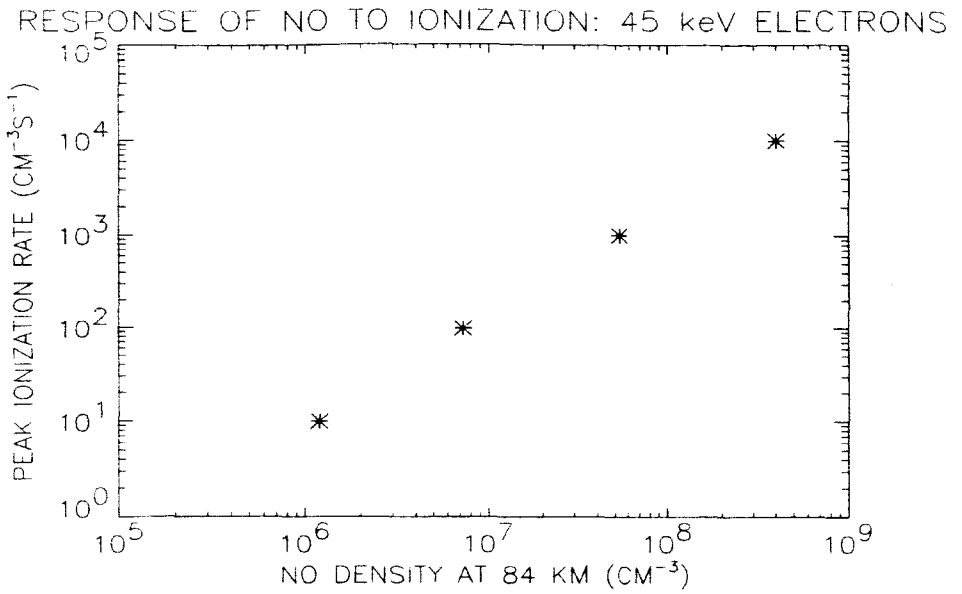

Figure 5.1. **Steady state 1-Dimensional model results for the amount of NO created at 84 km as the result of an ionization rate indicated.**

At a minimum, AIM needs to distinguish the amount of NO following strong disturbances from the low-level case. Because NO is so highly variable, it is not instructive to provide an accuracy and precision in percent. Instead, the minimum requirements are given in density. The HALOE database [Russell et al., 1993] shows high latitude NO densities in excess of 1×10^7 cm^{-3} near 90 km following a burst of medium energy electrons, which is consistent with model results in Figure 5.1. A minimum requirement for NO accuracy between 80-95 km of 1×10^7 cm^{-3} is therefore chosen.

Altitude Range: 80-95 km
Vertical Resolution: 5 km
Horizontal Resolution: 500 km
Temporal Resolution: 1 day
Accuracy: 1×10^7 cm^{-3}

8.2.5 Cosmic Dust

The measurement of dust from low earth orbit (LEO) can be used to estimate the deposition rate of cosmic material into the mesosphere. Dust particles pass through the region of the s/c altitude to the atmosphere in less than a minute and without any significant changes in their velocity vector or mass until they reach an altitude of 100 km. Entering the mesosphere, the particles swiftly exchange energy and momentum with the atmosphere due to the exponentially growing air density. The particles ablate in approximately 2 seconds and deposit most of their mass in the altitude region of 80-100 km [Kalashnikova et al., 2000]. The ablated material quickly (in minutes) re-condenses into nm size smoked particles [Hunten *et al.*, 1980] that might serve as nuclei for water condensation and hence could control the efficiency of NLC formation. The lifetime of nm sized smoke particles against coagulation and subsequent removal from the

mesopause region is short (days to weeks) compared with a PMC season (3 months). For this reason, the availability of smoke particles as nucleation sites in the mesosphere can be monitored in LEO and correlated to PMC occurrence frequency.

The latest observational evidence on PMCs from the Student Nitric Oxide Explorer (SNOE) indicates that there are dropouts in the PMC occurrence frequency on the order of a week (Figure 5.2). To explore whether PMC dropouts are due to the availability of cosmic dust, AIM needs to be sensitive to the incoming dust flux with count rates sufficiently high to distinguish weekly variability, which we take to be 10^2 counts/week.

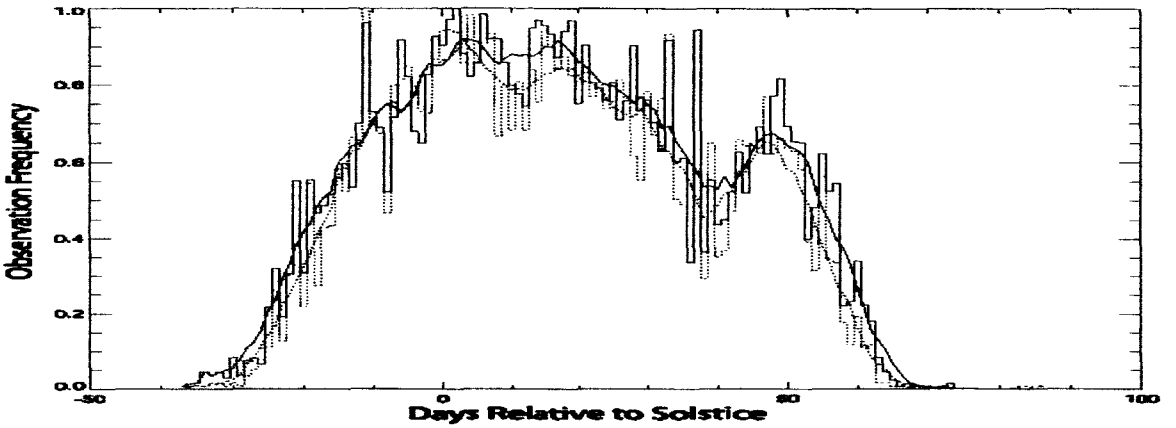

Figure 5.2. SNOE frequency of observations of Polar Mesospheric Clouds during the 1998 northern season at latitudes between 80 and 85°. Thin lines are daily measurements while thicker lines are a 9-day running smooth. The solid lines are for AIM measurements, the dotted lines are PM measurements.

Most of the mass to the Earth's atmosphere is delivered in the form of 100 μm radius particles, where the flux of these particles is less than 1 per week. It is expected, however, that the flux of smaller grains is significantly higher than this *["Orbital Debris: A Technical Assessment", National Academy Press, Washington, DC, 1995]*. We assume that during periods of high dust input rates the fluxes are elevated for all sizes, so that by monitoring the lowest end of the dust size distribution we will monitor the total dust influx as well. AIM needs to be sensitive to particles smaller than 1 μm in radius to build on previous work, which measured particles larger than this [Love and Brownlee, 1993]. The expected weekly and daily impact rates are shown in Figure 5.3 for a 900 cm^2 surface area detector along. The radii required for minimum science and for a goal are indicated.

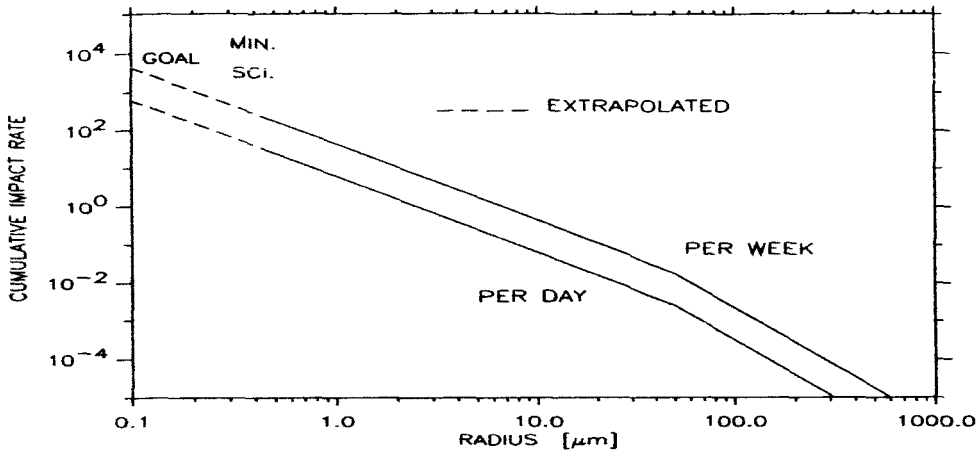

Figure 5.3. The expected cumulative impact rate as function of the particle radius for an integration period of 1 week and 1 day. The rates are for a 900 cm^2 surface area detector. In order to confidently notice a 10% level change in the dust input a minimum of 100 counts is needed (0.6-0.7 μm). At a minimum we must achieve this on a weekly time-scale. Our goal is to notice 10% variability on a daily basis. In order to achieve this, our threshold has to be lowered into the 0.2-0.3 μm range.

Altitude Range: S/C altitude
Vertical Resolution: N/A
Size range: <0.7 μm
Temporal Resolution: 1 week
Precision: 10%

8.2.6 Summary of Geophysical Parameters Required for Objective 5

	PMC Morphology		Temperature		Water Vapor		Nitric Oxide		Cosmic Dust	
	Min	Goal	Min	Goal	Min	Goal	Min	Goal	Min	Goal
Altitude Range (km)	81-85	75-95	81-85	75-95	81-85	75-95	80-95	80-130	S/C	
Vertical Resolution (km)	3	1	3	1	3	1	5	1	N/A	
Horizontal Resolution (km)	500	150	500	150	500	150	500	100	N/A	
Temporal Resolution	1 min.	12 s	1 day	1 min	1 day	1 min	1 day	1 hr	1 wk	1 day
Precision	56%	2%	±5 K	±1 K	50%	10%	1×10^7 cm^{-3}	1×10^6 cm^{-3}	10% (<0.7 μm)	10% (<0.2 μm)

9 Objective 6. Long-Term Mesospheric Change

9.1 Science Question

What is needed to establish a physical basis for the study of mesospheric climate change and its relationship to global change?

NLC occurrences have been increasing and mesospheric temperatures appear to have been declining over the last several decades. Our hypothesis is that PMC occurrence and change are sensitive indicators of global climate change. To test that hypothesis, AIM will provide a new understanding of why such clouds form and how they respond to short term environmental changes. By quantifying the roles of temperature, H_2O and dynamics in forming clouds and by assessing the role of extraterrestrial forcing, we will develop precision criteria for monitoring the upper mesospheric environment. Also, by validating the ability of a global chemical/ transport model to simulate the observed seasonal, latitudinal and N/S variations of PMC occurrences, we will develop the capability to do trend assessments. This approach is similar to that taken by 2D models for stratospheric ozone (World Meteorological Organization (WMO), 1999, chap. 12).

By "climate change" and "long-term" change, we mean any significant year-to-year changes (above the natural variability due to random day-to-day changes). For example, changes due to solar activity, to carbon dioxide increases, or methane increases fall under this definition. It does *not* include changes induced by an enhancement of medium energy electrons, a solar proton event or by a sporadic change in cosmic dust influx. Furthermore, it does not include interannual changes, such as those associated with the quasi-biennial oscillation of stratospheric wind. It is clear that with only a two-year time period, no *direct* measurements of long-term changes can be made. However, a two-year measurement set of PMC and the important forcing variables, combined with a validated model, will provide an unprecedented evaluation of past, present and future space changes of Polar Mesospheric Clouds. In turn, this will enable an assessment of the climatic changes in the atmospheric parameters themselves.

9.2 Required Geophysical Parameters

9.2.1 PMC Limb Brightness Distribution

The desired measurement is the presence or absence of a PMC, as a function of geographic location and time. A PMC detection requires a limb enhancement in the brightness or extinction of sunlight on the limb near the 83-km region. This effect needs to be several times larger than the noise level of the instrument, and any fluctuations in the brightness due to non-PMC causes.

This objective will require many hundreds of individual PMC measurements, grouped together according to their brightness, latitude, time within season, etc. This is because the statistical accuracy varies roughly as the inverse of the square root of the number of observations. PMC frequency (f) is a statistical quantity that may be defined in various ways, and depends upon the experimental parameters (such as wavelength, scattering angle, threshold of detection, etc.). It is usually defined as the ratio of the number of clouds observed over a specified geographical area, and a specified interval of time, divided by the number of observations. Typically, the area covers a 5-degree distance of latitude, or 5 degrees along the orbit track. This corresponds to about 550 km in the meridional direction. This choice is governed by the following: the line of sight is several hundred km (specifically, 227 km for a 1-km thick cloud and 321 km for 2-km thickness). Thus 5 degrees is a conservative choice for assuring independent (uncorrelated) measurement sets. In the east-west, or cross-track direction, the area will be the field of view. For example, for SME and SNOE this distance is about 35 km. Ideally the smallest time interval is

one day, or for a 100% data coverage, 15 to 16 orbits per day. However to minimize the effects of day-to-day variability, which is of no interest to seasonal or long-term climate changes, a 5-day interval is preferred. 5 days is long enough to considerably reduce the effects of day-to-day variations, but short enough not to distort the seasonal changes, which occur over a total PMC season of about 60 days.

In principle, it is difficult to define precisely the regions of "cloud" and "no-cloud", since there is always the possibility that the "no-cloud' region may simply be a "weak-cloud" region, undetected by the particular technique. However, if we define a standard threshold of detection, then any changes (above the uncertainty for a given season) from year to year must be real. f must be defined carefully to remove systematic influences, such as differing sensitivities and wavelengths between various instruments. This statistical measure of climate variability has been proven to be useful in comparing three different satellite data series (Shettle et al, 2002). In order to compare current or future measurements with historical and future measurements, we need to establish a method which is essentially *calibration independent*. Solar occultation measurements satisfy this objective, as they deal with a ratio of two measurements (a cloud measurement and a solar measurement). In the same way, we can also use data of PMC observed in passive solar scattering, or active lidar scattering if we use a ratio of two measurements. It has become standard procedure in lidar studies to report the ratio of the PMC back-scattered intensity to that of a cloud-free region at the same height; or in other words the ratio of the Rayleigh +Mie scattering to the Rayleigh scattering. This is called the *backscattering ratio* (BSR) in lidar parlance. For satellite measurements at the limb, this ratio (less one) is called the limb *scattering ratio*, or LSR. In the case of the solar extinction data from POAM, SAGE-II, HALOE and SOFIE, a similar ratio may be defined, the *extinction ratio*, ER. ER and BSR are closely related at visible and UV wavelengths, since the absorption (actual loss of energy within the particles) due to water-ice is negligible. Thus the attenuation of the solar signal at wavelengths shorter than about 1 micron is due solely to scattering. It is definitely not true for near-IR solar occulation measurements. Quantitatively relating the two quantities, ER and BSR, requires the size distribution of the optically-active particles. This is because the variation of scattering with angle is sensitive to the particle size, when the particle size is not small compared with the wavelength. The relationship between BSR and ER is very simple in the small-particle (Rayleigh) limit, in which the scattering phase function is a simple analytic function of scattering angle. However, for larger particles, the scattering phase function must be calculated by a rather complicated computer algorithm. Up to now, the basic assumption is that the Mie theory applies, which strictly is valid for spherical particles. However in practise, it has been shown that even if the particles are elongated or irregular ice crystals, they act as spheres up to equivalent spherical radii of about 0.1 micron. (Fortunately most ice particles are smaller than this.)

Visible lidar measurements have detected clouds as bright as BSR=500. Up to recently, the detection threshold for lidar measurements has been of the order of 5 to 10. UV satellite measurements have detected clouds with LSR of several hundred, and minimum values are of the order of 0.5. POAM has measured ER values up to 30 (these refer to low-latitude clouds) , with thresholds of about 4 to 5. Noise in the sky background signal can imitate a weak cloud, and unless there are several colors measured simultaneously, it is necessary to set the threshold to a value that excludes most positive (non-PMC) fluctuations in the background.

The cloud-free atmosphere can be readily identified if the scattering profile has a scale height, appropriate to the temperature of the mesopause region. Ideally, this is in the same common volume. It has been necessary to define the reference scattering level in a latitude zone that is known to be cloud-

free. For example, in the analysis of SME 265 nm data, Olivero and Thomas (1986) and Thomas and Olivero (1989) adopted the cloud-free standard to be the 50-55 degrees latitude zone. Thus it is necessary to assume that the horizontal variation of the atmospheric density is not significant between the reference region and the cloud region. The error is probably small in the adjacent 60-degree zone, but will increase as the distance from the reference region increases, for example at the pole. This is because the temperature (and therefore density) usually decreases toward the pole. It is possible to reduce this error, by using an atmospheric model of density to correct for this gradient, for example the MSIS model.

A second consideration is the cloud detection algorithm. The method used in the SME and SNOE analyses of limb data is to use the signals in two simultaneous and independent measurements, at two different wavelengths (for SME, 265 nm and 296 nm). It is important to rule out "false clouds", those which mimic clouds through a purely random coincidence in which the noise in both channels are large and positive. By using the conservative criterion that a real cloud must exceed 3 standard deviations in both channels, nearly all (0.03% in the case of uncorrelated noise in both channels) false clouds can be eliminated from the data analysis. In addition, the clouds must occur in a restricted region of tangent height, typically 75-100 km. For the SME UVS, these criteria ruled out all clouds weaker than about twice the 83-km background. More recently, we have been able to reduce the criterion from 3-sigma to 2-sigma, in which case we can reliably detect clouds down to values of SR-1 as small as 70% of the Rayleigh background.

Lidar techniques rely upon the height profile of the returned signal to determine whether a cloud is present or not. Due to their greater height resolution, lidar can rely upon there being a local maximum in the 75-100 km region. Up to now, the frequency of occurrence of ALOMAR (an aeronomy observatory in Andenes, Norway) lidar observations have been somewhat less than that of SME at 69N, probably because of their higher threshold. With recent improvements, the ALOMAR LIDAR is now capable of detecting PMC BSR's to thresholds comparable to the background itself, even in daytime. (It should also be noted that because of the differing spectral dependences of the Mie and Rayleigh scattering, a BSR in the visible is higher than in the UV, by a factor of about two.) This will be an important consideration in tying the AIM measurements to ground-based measurements. This of course assumes that ALOMAR will continue its daytime monitoring of PMC, which is not at all assured, even through the AIM period. At this time, no other LIDAR has daylight capability, but the Greenland LIDAR is being upgraded, and may soon have this ability.

With reference to the importance of satellite measurements of frequency, f in global change studies, if defined carefully for some standard set of conditions (for example, the UV wavelengths of SME, 265nm and 296 nm), f could be an important index of global change assessment. Its advantages are (1) that it can be defined as a globally-extensive quantity, appropriate for large-scale (zonally-averaged) studies, and therefore relatively independent of local influences, such as sporadic gravity wave activity; (2) With the appropriate corrections for wavelength and scattering angle, f can be compared with ground-based (either visual or preferably lidar) measurements taken over consecutive summers over long periods of time, and with past satellite measurements (Shettle et al, 2002); (3) Because most PMC are dim, and expected to be close to Rayleigh-like in their scattering properties, occurrence frequency is relatively free of errors in scattering angle and wavelength corrections; (4) it is easy to understand as a "cloudiness" index, and therefore easy to explain to the public.

Disadvantages of the cloud frequency are: (1) when the frequency approaches unity, it becomes useless. This occurs near the pole during the heart of the PMC season. Even for frequencies > 50%, the index begins to lose its value as a climate index: (2) Because it is weighted toward the more numerous dim clouds, it essentially ignores changes that might be occurring in the bright cloud category (this latter problem is avoided if the cumulative frequency is used, the so-called g-distribution- see next section); (3) No one has yet related the ground-based quantity (the number of clouds observed per season) to the satellite-based frequency of occurrence.

With respect to the accuracy of the backscattering ratio (or in the case of solar extinction, the extinction ratio), the only important requirement is that the photon-counting detector have sufficient signal-to-noise ratio for a 10% accuracy on a weak cloud (say, LSR=2). For higher LSR, of course, the accuracy will improve. Because PMC are optically-thin, the signal is proportional to the scattering optical depth, and thus it is easy to estimate the overall error in the mean scattered intensity. Because we are dealing with the scattering ratio as the primary data, we must divide the cloud intensity by the cloud-free 83-km signal. Thus the overall error in LSR is dominated by the error in this (small) signal. However, this too can be reduced, since the density variations throughout an orbit and throughout the season (at a fixed latitude) are expected to be small, but probably not less than 10%. To be conservative, it is estimated that the limiting accuracy of the daily-averaged LSR, or ER, is probably ~10%. It is estimated that gravity wave and planetary wave variability will cause the overall frequency of a given season to be at least 15%. Thus any change from season to season in the LSR deemed to be of climate significance will exceed 15%.

The considerations above apply only to limb measurements. UV imaging is an entirely different type of measurement, since the background is not the 83-km Rayleigh scattering, but the 50-km Rayleigh scattering. *Thus it is impossible to determine the LSR directly from imaging data.* However, it is still possible to study latitudinal, seasonal and hemispherical changes in a different ratio, that of the height-integrated intensity, divided by the 50-km intensity, R. This is a quantity, that like LSR or ER, will be independent of the absolute calibration. Unfortunately, this ratio will be dependent upon the 50-km ozone density, which itself has systematic variations with latitude, season, etc. *Therefore R is not a good climate indicator of PMC changes.* Thus the accuracy requirements for LSR and ER, and thus frequency of occurrence is determined solely by the limb experiments.

As far as vertical resolution of the limb experiments is concerned, it is important to resolve the rather narrow spike-like character of an "edge-on" PMC limb profile. This spike is a result of the typical PMC thickness 1 to 2 km. Also, satellite measurements show that the vertical variation of PMC height around the mean is 1.5-3 km. A cloud can occur as low as, in principal, the surface on the limb profile (this is an *apparent* height, and is due to a foreground, or background cloud). It can occur up to as high as 85 km, perhaps occasionally still higher. A broad field of view, such as that of the SME and the SNOE UVS, effectively reduces the sensitivity of the measurement, by reducing the peak intensity. A 1-km field of view will reduce the peak intensity of a 1-km thick cloud (compared to an infinitesimal fov) by 30%. Thus this design is probably an acceptable compromise, given the other uncertainties in determining the scattering ratio, and given the fact that smaller fields of view give a diminishing return (for example, a 0.5 km fov causes a smearing of 20%). This requirement also imposes a minimum data rate, because of the need to oversample the data, by at least a factor of two. That is, at least two samples need to be taken while the limb scan is covering 1 km on the limb.

As far as horizontal resolution is concerned, because of the considerable line-of-sight smearing, if the samples are closely spaced, the data tends to be redundant, ie. is auto-correlated. A maximum separation is 227 km, which is the line of sight distance through a 1-km thick PMC. This corresponds to about 2 degrees along the orbit. The goal is about 200 km, which helps dictates the sampling rate, and a minimum value is 500 km.

The g-distribution. This concept was introduced by Thomas (1995) in an attempt to compare year-to-year variations of PMC detected by the satellite sensors on board SME and SBUV. It has also been helpful in comparing PMC observed by POAM II, WINDII and SME. The determination of g requires an accurate determination of the PMC limb brightness of PMC, in the case of a limb-scattering measurement, and of the extinction optical depth, in the case of a solar occultation measurement. The same ideas presented below apply to both. The g-distribution was defined by Shettle et al. (2002) as the cumulative number of PMC brighter than a certain value of extinction ratio, ER, divided by the total number of observations. The value of g at the detection threshold value ER0, is thus equal to the frequency of occurrence f, that is, g(ER0)=f. g(ER) is proportional to the number of clouds brighter than ER. For any satellite mission for 15 orbit per day coverage, the statistics are generally sufficient to define g as a function of latitude, in five degree increments. Because of the greater information in the g-distribution (typically this would be twenty points distributed over the full range of ER, from unity up to perhaps 100 or even more), the data over the full season should be used. Ideally, they should all be at the same latitude, within 5 degrees. The use of ER, rather than BSR, is required because of the fact that the scattered intensity of the brighter clouds is a sensitive function of scattering angle. In order to make the conversion from BSR to ER, we require the Mie scattering phase function, and hence the mean particle size, as described above.

Since both bright and dim clouds increase in numbers with latitude, g-distributions as a function of latitude show a systematic increase of the "tail" of the distribution with increasing latitude, and also an increase at the threshold value. From year to year, the SBUV observations of PMC in the nadir showed a significant increase in the number of bright clouds from solar maximum to solar minimum conditions (Thomas et al, 1991; DeLand, 2002). This is consistent with previous results from ground-based sightings of NLC (Gadsden, 1998)

The g-distribution carries much more information than the frequency of occurrence. It requires a determination of the peak PMC optical depth, ratioed to the background optical depth at the same height. The price that one pays for this increased information is that an entire season of data must be used. This is particularly true of the lower latitudes, where the cloud frequency is quite low. The advantages of the g-distribution are: (1) comparisons at all intensity groups may be made from season to season. Thus if for example, only the number of very bright clouds were to have a systematic change from one season to the next, or between hemispheres, this shows up in the "tail" of the distribution. Increase of only the bright cloud numbers from year to year is probably not detectable in the frequency of occurrence, because this is weighted toward the more numerous weak clouds; (2) unlike the frequency of occurrence, the g-distribution saturates for weak clouds, but is still meaningful at the higher values of ER. It is obvious that the mean extinction ratio is the first moment of the g-distribution, and hence the g-distribution carries all the important statistical information about the global behavior of PMC. *It is the preferred index to examine long-term globally-extensive changes from satellite measurements.* The accuracy requirements for the g-distribution are the same as for the frequency of occurrence.

Altitude range:80-85 km
Vertical Resolution:1 km
Horizontal resolution:500 km
Temporal Resolution: 1week
Accuracy: ± 15%
Precision: ± 10%

9.2.2 Water Vapor

The concurrent measurements of water vapor (H_2O) and temperature (T) will be key to the AIM mission objectives, both those of microphysics and of global change. The relationships of PMC, T and H_2O will be established from several thousands of cloud events over a wide variety of values of T and H_2O. Both temperature (atmospheric cooling due to increased greenhouse gases) and changes in the middle atmospheric humidity (due to enhanced entry of water vapor into the stratosphere, combined with atmospheric methane increases) have been suggested as the causative factors in the changes observed in both NLC ground-based sightings, and recently satellite measurements of PMC. In addition, AIM will be able to isolate the importance of cosmic dust influences. The model predictions of these relationships will be tested, and if successfully verified, will be used in assessing the long-term changes of PMC as T, H_2O. varies in time within the season, varies with latitude and from one hemisphere to the other. The climate indices mentioned above (frequency of occurrence and the g-distribution) will be ultimately tied to the forcing variables through statistical correlations and detailed modeling. PMC will be verified as a legitimate climate index in its own right. It can then be used to assess the changes that have occurred in the atmosphere over the past 117 years, and be used as a predictor for future saturation conditions within the summertime mesosphere.

For this objective, which is concerned with long term changes, water vapor does not need to be determined with any greater resolution, precision, or accuracy than will be required for the prior objectives. In particular if the microphysics objective is achieved, then the long-term change objective will also be successful.

The numerical values below are determined by the following: The 200 km resolution as a goal for all measurements of concern to upper atmospheric climate change recognizes the basic horizontal smearing of limb measurements. Since most past measurements, and many future measurements (including AIM) will be conducted at the limb, this is the goal. The 500 km value is the grid size (5 degrees) adopted previously for SME and SNOE climatology. The vertical resolution for limb measurements is dictated by the need to resolve the PMC "spike" at the limb to prevent the field-of-view smearing from being worse than 30%. The minimum of 2 km still achieves the goal of separating the clouds from the background, but with a reduced sensitivity. Nevertheless, it exceeds SME and SNOE fields of view. The accuracy and precision of the PMC scattering ratio (and thus the derived quantities of f and g) is dictated by the fact that the 83-km background will have an inherent error of 10%. The 15% value is determined by the assessment that any significant year to year change at a given latitude must be at least this large, to exceed that caused by natural variability due to gravity waves and planetary waves.

Altitude Range: 81-85 km
Vertical Resolution: 3 km
Horizontal Resolution: 500 km
Temporal Resolution: 1 day
Precision: 50%

9.2.3 Temperature

The concurrent measurements of water vapor (H_2O) and temperature (T) will be key to the AIM mission objectives, both those of microphysics and of global change. Both temperature changes and changes in the middle atmospheric humidity have been suggested as the causitive factors in the changes observed in both NLC ground-based sightings, and recently satellite measurements. The relationships of PMC, T and H_2O will be established from several thousands of cloud events over a wide variety of values of T and H_2O. For this objective, which is concerned with long term changes, temperature does not need to be determined with any greater resolution, precision, or accuracy than will be required for the prior objectives. In particular if the microphysics objective is achieved, then the long-term change objective will also be successful.

Altitude range: 81-85 km
Vertical Resolution: 3 km
Horizontal Resolution: 500 km
Temporal Resolution: 1 day
Accuracy : ±5 K

9.2.4 Summary of Geophysical Parameters Required for Objective 6

	PMC Limb Brightness and/or Extinction Distr.		Temperature		Water Vapor	
	Min	Goal	Min	Goal	Min	Goal
Altitude Range (km)	81-85	75-95	81-85	75-95	81-85	75-95
Vertical Resolution (km)	3	1	3	1	3	1
Horizontal Resolution (km)	500	150	500	150	500	150
Temporal Resolution	1 min.	12 s	1 day	1 min	1 day	1 min
Precision	15%[1]	10%	±5 K	±1 K	50%	10%

[1] This value applies to PMC well above the detection threshold

References

Akmaev, R. A. A prototype upper-atmospheric data assimilation scheme based on optimal interpolation, 1, Theory, *J. Atmos. Terr. Phys., 61*, 491-504, 1999.

Allen, M., J.I. Lunine, and Y.L. Yung, The Vertical Distribution of Ozone in the Mesosphere and Lower Thermosphere, *J. Geophys. Res.*, 89, 4841-4872, 1984.

Avery S. K., R. A. Vincent, A. Phillips, A. H. Manson, G. Fraser, High-latitude tidal behavior in the mesosphere and lower thermosphere, *J. Atmos. Terr. Phys., 51*, 595-608, 1989.

Azeem, S. M. I., T. L. Killeen, R. M. Johnson, Q. Wu, and D. A. Gell, Space-time analysis of TIMED Doppler interfereometer (TIDI) measurements, *Geophys. Res. Lett., 27*, 3297-3300, 2000.

Bacmeister, J. T., S. D. Eckermann, A. Tsias, K. S. Carslaw, and T. Peter, Mesoscale temperature fluctuations induced by a spectrum of gravity waves: A comparison of parameterizations and their impact on stratospheric microphysics, *J. Atmos. Sci., 56*, 1913-1924, 1999.

Brasseur, G. and S. Solomon, Aeronomy of the Middle Atmosphere (Reidel, Dordrecht, Netherlands, 1986).

Carbary, J. F., D. Morrison, and G. J. Romick, Transpolar structure of polar mesospheric clouds, *J. Geophys. Res., 105*, 24,763-24,769, 2000.

Carbary, J.F., et al., Hemispheric comparison of PMC altitudes, *Geophys. Res. Lett.*, in Press, 2001.

Codrescu, M.V. et al., Medium energy particle precipitation influences on the mesosphere and lower thermosphere, *J. Geophys. Res.*, 102, 19977-19987, 1997.

Conway, R.R. et al., Satellite measurements of hydroxyl in the mesosphere, *Geophys. Res. Lett.*, 23, 2093-2096, 1996.

Coy, L., T. Hogan, Y.-J. Kim, S. D. Eckermann, and J. McCormack, Extending NOGAPS (Navy Operational Global Atmospheric Prediction System) to include the middle atmosphere, paper to be presented at AGU Spring Meeting, Washington, DC, 28-31 May, 2002.

DeLand, M.T., E. P. Shettle, G. E. Thomas and J. J. Olivero, SBUV Observations of PMCs Over Two Solar Cycles, *J. Geophys. Res.*, submitted, 2002.

Eckermann, S. D., D. E. Gibson-Wilde, and J. T. Bacmeister,, Gravity wave perturbations of minor constituents: a parcel advection methodology, *J. Atmos. Sci., 55*, 3521-3539, 1998.

Fetzer, E. J., and J. C. Gille, Gravity wave variance in LIMS temperatures. Part I: variability and comparison with background winds, *J. Atmos. Sci., 51*, 2461-2483, 1994.

Forbes, J. M., N. A. Makarov, Y. I. Portnyagin, First results from the meteor radar at South Pole - a large 12-hour oscillation with zonal wave-number one, *Geophys. Res. Lett., 22*, 3247-3250,1995.

Frame, D. J., B. N. Lawrence, G. J. Fraser, R. A. Vincent, and A. Dudhia, A new technique for evaluating mesospheric momentum balance utilizing radars and satellite data, *Ann. Geophysicae, 18*, 478-484, 2000.

Gadsden, M., Noctilucent clouds seen at 60°N: origin and development, *J. Atmos. Sol-Terr. Phys., 60*, 1763-1772, 1998.

Gadsden, M., Letter to the Editor: An early observation of noctilucent cloud?, J. British Astro. Asso., 109, 354, 1999.

Gadsden, M., Structure in polar mesospheric clouds seen from a geostionary spacecraft, *Geophys. Res. Lett., 27*, 3671-3673, 2000.

Gerrard, A. J., T. J. Kane, and J. P Thayer, Noctilucent clouds and wave dynamics: observations at Sondrestrom, Greenland, *Geophys. Res. Lett., 25*, 2817-2820, 1998.

Haurwitz, B. and B. Fogle, Wave forms in noctilucent clouds, Deep-Sea Research and Oceanograph. Abstracts (Permagon Press, Great Britain) 16, Suppl., 85-95, 1969.

Huaman, M. M., and B. B. Balsley, Differences in near-mesopause summer winds, temperatures, and water vapor at northern and southern latitudes as possible causal factors for inter-hemispheric PMSE differences, *Geophys. Res. Lett., 26*, 1529-1532, 1999.

Hunten, D.M., P.R. Turco and O.B. Toon, Smoke and dust particles of meteoric origin in the mesosphere and stratosphere, *J. Atmos. Sci.*, 37, 1342-1356, 1980.

Jensen and Thomas, JGR, 1994.

Keckhut, P., A. Hauchecorne, M. L., Chanin, Midlatitude long-term variability of the middle atmosphere - trends and cyclic and episodic changes, *J. Geophys. Res., 100*, 18,887-18,897, 1995.

Kirkwood, S., et al., The 1997 PMSE season - its relation to wind, temperature and water vapour, *Geophys. Res. Lett.*, 25, 1867-1870, 1998.

Klostermeyer, JGR, 1998.

Lieberman, R. S., The gradient wind in the mesosphere and lower thermosphere, *Earth Planets Space, 51*, 751-761, 1999.

Love, S.G. and D.E. Brownlee, A direct measurement of the terrestrial mass accretion rate of cosmic dust, *Science*, 262, 550-553, 1993.

Lübken, F.-J. and U. von Zahn, Thermal structure of the mesopause region at polar latitudes, *J. Geophys. Res.*, 96, 20841, 1991.

Lübken, F.-J., Thermal structure of the Arctic summer mesosphere, *J. Geophys. Res., 104*, 9135-9149, 1999.

Lübken, F.-J., M. J. Jarvis, and G. O. L. Jones, First in situ temperature measurements at the Antarctic summer mesopause, *Geophys. Res. Lett., 26*, 3581-3584, 1999.

Luo, Z. G., D. C. Fritts, R. W. Portmann, and G. E. Thomas, Dynamical and radiative forcing of the summer mesopause circulation and thermal structure, 2, seasonal-variations, *J. Geophys. Res., 100*, 3129-3137, 1995.

McLandress, C., M. J. Alexander, and D. L. Wu, Microwave limb sounder observations of gravity waves in the stratosphere: a climatology and interpretation, *J. Geophys. Res., 105*, 11,947-11,967, 2000.

Merkel, A. W.; Thomas, G. E.; Palo, S. E.; Bailey, S. M., Observations of the 5-day planetary wave in PMC measurements from the Student Nitric Oxide Explorer Satellite, *Geophys. Res. Lett., 30(4)*, 1196, doi:10.1029/2002GL016524, 2003.Oberheide, J., M. E. Hagan, W. E. Ward, M. Riese, and D. Offermann, Modeling the diurnal tide for the Cryogenic Infrared Spectrometers and Telescopes for the Atmosphere (CRISTA) 1 time period, *J. Geophys. Res., 105*, 24,917-24,929, 2000.

Olivero, J.J., and G.E.Thomas, Climatology of Polar Mesospheric Clouds ,J. Atmospheric Sciences, 43, 1263-1274, 1986.

Palo, S. E., R. G. Roble, and M. E. Hagan, Middle atmosphere effects of the quasi-two-day wave determined from a General Circulation Model, *Earth Planets Space, 51*, 629-647, 1999.

Pawson, S., K. Kruger, R. Swinbank, M. Bailey, and A. O'Neill, Intercomparison of two stratospheric analyses: Temperatures relevant to polar stratospheric cloud formation, J. Geophys. Res., 104, 2041-2050, 1999.

Preusse, P., S. D. Eckermann and D. Offermann, Comparison of global distributions of zonal-mean gravity wave variance inferred from different satellite instruments, *Geophys. Res. Lett., 27*, 3077-3080, 2000.

Preusse, P., A. Dörnbrack, S. D. Eckermann, M. Riese, B. Schaeler, J. T. Bacmeister, D. Broutman, and K. U. Grossmann, Space-based measurements of stratospheric mountain waves by CRISTA, 1, Sensitivity, analysis method, and a case study, *J. Geophys. Res., 107(D23)*, 8178, 10.1029/2001JD000699, 2002.Rees, D, U. von Zahn, G. von Cossart, K. H. Fricke, W. Eriksen, and J. A. McKay, Daytime lidar measurements of the stratosphere and mesosphere at the ALOMAR Observatory, *Adv. Space Res., 26(6)*, 893-902, 2000.

Reid, G., Ion chemistry of the cold summer mesopause region, *J. Geophys. Res.*, 94, 14,653-14,660, 1989.

Roble, R.G. and E.C. Ridley, A thermosphere-ionosphere-mesosphere-electrodynamics general circulation model (TIME-GCM): Equinox solar cycle minimum simulations (300-500 km), *Geophys. Res. Lett.*, 21, 417-420, 1994.

Russell, J.M. III et al., The Halogen Occultation Experiment, *J. Geophys. Res.*, 98, 10777, 1993.

Russell, J.M. III et al., Aeronomy of Ice in the Mesosphere: AIM, 2001.

Schmidlin F. J., H. S. Lee, and W. Michel, The inflatable sphere - a technique for the accurate measurement of middle atmosphere temperatures, *J. Geophys. Res., 96*, 22,673-22,682, 1991.

Seele, C. and P. Hartogh, Water vapor of the polar middle atmosphere: Annual variation and summer mesosphere conditions as observed by ground-based microwave spectroscopy, *Geophys. Res. Lett.*, 26, 1517-1520, 1999.

Shettle, E. P., G. E. Thomas, J. J. Olivero, W. F. J. Evans, D. J. Debrestian and L. Chardon, Three satellite comparison of Polar Mesospheric Clouds: Evidence for Long-term Change, J. Geophys. Res., in press, 2002.

Siskind, D.E., et al., The response of thermospheric nitric oxide to an auroral storm, 2. Auroral Latitudes, *J. Geophys. Res.*, 94, 16899, 1989.

Siskind, D.E. and M.E. Summers, Implications of Enhanced Mesospheric Water Vapor Observed by HALOE, *Geophys. Res. Lett.*, 25, 2133-2136, 1998.

Siskind, D. E., S. D. Eckermann, J. P. McCormack, M. J. Alexander, and J. T. Bacmeister, Hemispheric differences in the temperature of the summertime stratosphere and mesosphere, *J. Geophys. Res., 108(D2)*, 4051, doi:10.1029/2002JD002095, 2003.States, R. J., and C. S. Gardner, Thermal structure of the mesopause region (80-105 km) at 40°N latitude, part I: seasonal variations, *J. Atmos. Sci., 57*, 66-77, 2000.

Strahan S.E., et al., Long-lived tracer transport in the Antarctic stratosphere, *J. Geophys. Res.*, 101, 26615-26629, 1996.

Sugiyama, T. et al., Oscillations in polar mesospheric summer echoes and bifurcation of noctilucent cloud formation, *Geophys. Res. Lett.*, 23, 653-656, 1996.

Summers, M.E., R.R. Conway, D.E. Siskind, R. Bevilacqua, D.F. Strobel, and S. Zasadil, Mesospheric HO_x Photochemistry: Constraints from concurrent measurements of OH, H_2O, and O_3, *Geophys. Res. Lett.*, 23, 2097-2100, 1996.
Summers, M.E. et al., The Seasonal Variation of Middle Atmospheric CH4 and H_2O with a new chemical-dynamical model, *J. Geophys. Res.*, 102, D3, 3503-3526, 1997.

Summers, M.E., R.R. Conway, D.E. Siskind, M.H. Stevens, D. Offermann, M. Riese, P. Preusse, D.F. Strobel, and J.M. Russell III, Implications of Satellite OH Observations for Middle Atmopsheric H_2O and Ozone, *Science*, 277, 1967-1970, 1997.

Summers, M.E., and D.E. Siskind, Surface Recombination of O and H_2 on Meteoric Dust as a Source of Mesospheric Water Vapor, *Geophys. Res. Lett.*, 26, 1837-1840, 1999.

Summers, M.E. and R.R. Conway, Insights into Middle Atmospheric Hydrogen Chemistry from Analysis of MAHRSI OH Observations, AGU Monograph *Atmospheric Science Across the Stratopause*, 117-130, 2000.

Summers, M.E., R.R. Conway, C.R. Englert, D.E. Siskind, M.H. Stevens, J.M. Russell III, L.L. Gordley, M.J. McHugh: Discovery of a Water Vapor Layer in the Arctic Summer Mesosphere, Geophys. Res. Lett., 28, 3601-3604, 2001.

Thomas, G.E. and J.J. Olivero, Climatology of Polar Mesospheric Clouds. 2. Further analysis of Solar Mesosphere Explorer Data, J. Geophys. Res., 94, 14,673-14,68, 1989

Thomas, G.E., Mesospheric clouds and the physics of the mesopause region, Rev. Geophys., 29, 553-575, 1991.

Thomas, G.E., R.D. McPeters, and E.J. Jensen, Satellite Observations of Polar Mesospheric Clouds by the Solar Backscattered Ultraviolet Spectral Radiometer: Evidence of a Solar Cycle Dependence J. Geophys. Res., 96, 927-939, 1991.

Thomas, G.E., Climatology of Polar Mesospheric Clouds: interannual variablitity and implications for long-term trends, in The Upper Mesosphere and Lower Thermosphere: A Review of Experiment and Theory, Geophysical Monograph 87, 185-200, 1995.

Thomas, G.E., Z. Chen, and J.J. Olivero, Optical and physical properties of polar mesospheric clouds inferred from Solar Mesospheric Explorer limb sounding data (1981-1986), presented at the AGU meeting, San Francisco, December 2000.

VonZahn, U, J. Hoffner, V. Eska, and M. Alpers, The mesopause altitude: Only two distinctive levels worldwide?, *Geophys. Res. Lett., 23*, 3231-3234, 1996.

Wickwar, V. B., M. J. Taylor, J. P Herron, and B. A. Martineau, Visual and lidar observations of noctilucent clouds above Logan, Utah, at 41.7°N, manuscript in preparation, 2001.

Williams C. R., and S. K. Avery, Analysis of long-period waves using the mesosphere-stratosphere-troposphere radar at Poker Flat, Alaska, *J. Geophys. Res., 97*, 20,855-20,861, 1992.

Witt, G., Height, structure and displacement of noctilucent clouds, Tellus XIV, 1-18, 1962.

Witt, G., The Nature of Noctilucent Clouds, Space Research, 9, 157-169, 1969.

WMO, Global Ozone Research and Monitoring Project – Report No.44, *Scientific Assessment of Ozone Depletion: 1998*, 1999.

Woodman, R. J., B. B. Balsley, F. Aquino, L. Flores, E. Vazquez, M. Sarango, M. M. Huaman, and H. Soldi, First observations of polar mesosphere summer echoes in Antarctica, *J. Geophys. Res., 104*, 22,577-22,590, 1999.

Wu, D.-L., and J. W. Waters, Observations of gravity waves with the UARS Microwave Limb Sounder, in *Gravity Wave Processes: Their Parameterization in Global Models*, NATO ASI Series, K. Hamilton ed., Springer-Verlag, Berlin, *I 50*, 103-120, 1997.